MEDICAL UNIVERSITY "PROF. DR. PARASKEV STOYANOV"VARNA
FACULTY OF MEDICINE
DEPARTMENT OF PHYSIOLOGY AND PATHOPHYSIOLOGY
TEACHING SECTOR OF PATHOPHYSIOLOGY

Dr. Diyana Asparuhova Kyuchukova

STUDY OF THE RELATIONSHIP BETWEEN OBESITY AND CARDIOVASCULAR DAMAGE IN AN EXPERIMENTAL MODEL OF METABOLIC SYNDROME

ABSTRACT

of the dissertation for the award of the educational and scientific degree of
DOCTOR (PhD)

Scientific Supervisor:
Assoc. Prof. Dr. Kameliya Zhechkova Bratoeva, MD

Varna, 2025

The dissertation comprises a total of 170 pages and is illustrated with 74 figures and 5 tables. A total of 445 literature sources are cited, of which 1 is in Cyrillic and 444 are in Latin script.

The dissertation was discussed, accepted, and approved for defense before a scientific jury by the Extended Departmental Council of the Department of Physiology and Pathophysiology at the Medical University "Prof. Dr. Paraskev Stoyanov" – Varna on 02 December 2025.

The public defense of the dissertation will take place on:

05 March 2026 at the Medical University of Varna – Auditorium III, at 14:00, at an open session of a scientific jury composed of:

External members:

1. Prof. Dr. Blagoy Ivanov Marinov, MD, PhD – habilitated in Professional Field 7.1. Medicine, Medical University of Plovdiv
2. Prof. Dr. Aneliya Aleksandrova Dimitrova, MD, PhD – habilitated in Professional Field 7.1. Medicine, Medical University of Pleven
3. Assoc. Prof. Dr. Armine Vardani Grigoryan, MD, PhD – habilitated in Professional Field 7.1. Medicine, Medical University of Pleven

Internal members:

1. Prof. Dr. Margarita Stefanova Velikova, MD, PhD – habilitated in Professional Field 7.1. Medicine, Medical University of Varna
2. Assoc. Prof. Dr. Radko Zlatkov Radev, MD, PhD – habilitated in Professional Field 7.1. Medicine, Medical University of Varna

Alternate external member:

1. Assoc. Prof. Dr. Krasimir Ginev Kostov, MD, PhD – habilitated in Professional Field 7.1. Medicine, Medical University of Pleven

Alternate internal member:

1. Prof. Dr. Zlatislav Stoyanov Dimitrov, MD, PhD – habilitated in Professional Field 7.1. Medicine, Medical University of Varna

The materials related to the defense of the dissertation have been published on the website of the Medical University "Prof. Dr. Paraskev Stoyanov" – Varna and are available at the Department of Physiology and Pathophysiology / Teaching Sector of Pathophysiology at the Medical University "Prof. Dr. Paraskev Stoyanov" – Varna.

CONTENTS

ABBREVIATIONS

ATP	adenosine triphosphate
ROS	reactive oxygen species
VAT	visceral adipose tissue
HFD	high fructose diet
ED	endothelial dysfunction
ET-1	endothelin - 1
DM	diabetes mellitus
BMI	body mass index
MS	metabolic syndrome
OS	oxidative stress
SAT	subcutaneous adipose tissue
AGEs	advanced glycation products
CAT	catalase
CPT1A	carnitine palmitoyiltransferase 1A
CRP	C-reactive protein
DNL	de novo lipogenesis
eNOS	endothelial nitric oxide synthase
GPx	glutathione peroxidase
HFCS	high fructose corn syrup
LDL, VLDL	low-density and very low-density lipoproteins
MHO	metabolically healthy obesity
NADPH-OX	Nicotinamide adenine dinucleotide phosphate oxidase
Nec-1	necrostatin - 1
NF-κB	nuclear factor kappa B
PVAT	perivascular fat tissue
RIP 1, RIP 3	Receptor-interacting protein kinase
SAM, S-AMe	S-adenosine methionine
SOD	superoxide dismutase
SREBP-1c	sterol regulatory binding protein-1c
TNF-α	tumor necrosis factor α
VCAM-1	vascular adhesion molecule -1
VEGF	vascular endothelial growth factor
VSMCs	vascular smooth muscle cells

I. INTRODUCTION

Nowadays, global obesity has reached unprecedented levels and represents one of the most significant challenges facing public health in the 21st century (WHO, 2022). The prevalence of this condition has escalated rapidly over the past 60 years. According to WHO data from 2022, 2.5 billion adults (aged 18 and over) were overweight, of whom 890 million live with obesity. At the same time, current treatment methods remain insufficiently effective.

The Obesity Medical Association (OMA) defines obesity as a chronic, multifactorial, relapsing, and neurobehavioral disease in which an increase in body fat leads to adipose tissue dysfunction and a range of adverse consequences for the human body. Obesity, as a complex health problem, can be influenced by various factors, including genetic predisposition, lifestyle, and dietary choices (Almoraie et al., 2024). Furthermore, literature data indicate that obesity directly contributes to the development of various cardiovascular risk factors, such as dyslipidemia, type 2 diabetes mellitus, atherosclerosis, and arterial hypertension, which are core components of metabolic syndrome, and leads to the development of cardiovascular diseases and mortality, independent of other cardiovascular risk factors (Powell-Wiley TM et al., 2021). Despite numerous studies, the exact reasons for this alarming increase remain unclear. It has been established that endothelial dysfunction, insulin resistance (IR), chronic inflammation, and oxidative stress (OS) are particularly important in the pathogenesis of obesity-associated cardiovascular diseases, which necessitates more in-depth research aimed at improving patients' quality of life.

Oxidative stress is a key factor in the pathogenesis of cardiovascular diseases, as it leads to endothelial dysfunction, lipid oxidation, vascular inflammation, and the formation of atherosclerotic plaques (Lugrin et al., 2014). Another critically important issue is the impact of OS on various aspects of the metabolic profile in patients with obesity. Excessive accumulation of reactive oxygen species (ROS) in adipocytes during obesity leads to the development of adipocyte dysfunction, or so-called "adipose tissue dysfunction," characterized by altered adipokine secretion and changes in adipocyte size and number (Polkinghorne et al., 2023). This dysfunction is associated with a reduced capacity of subcutaneous adipose tissue to store energy and increased ectopic fat deposition in tissues such as visceral adipose tissue, liver, and skeletal muscle (Tan et al., 2008). It has been found that visceral adipose tissue, in particular, significantly increases cardiovascular risk and leads to various metabolic disturbances in patients with obesity, highlighting the need to identify strategies to prevent or suppress the progression of oxidative stress through appropriate therapeutic interventions.

Dietary antioxidants have attracted considerable attention as effective means to combat oxidative stress and obesity-associated cardiometabolic disturbances. Various contemporary studies have explored in depth their anti-inflammatory properties and their involvement in regulating energy metabolism by enhancing thermogenesis and increasing resting energy expenditure. Dietary antioxidants also reduce oxidative stress and improve insulin sensitivity,

which are key factors in maintaining a healthy body weight (Almoraie et al., 2024).

Excess body weight and the accumulation of intra-abdominal visceral adipose tissue increase the risk of developing a range of cardiovascular damages, whose phenotypic expression and progression are more severe in this metabolic context. Changes in the immune system, along with increased secretion of hormones and cytokines from adipose tissue, in turn, stimulate chronic inflammation and create a pro-carcinogenic microenvironment (Blüher et al., 2019). Therefore, the early identification of inflammatory and endothelial biomarkers may facilitate timely intervention to prevent the progression and complications of obesity-related cardiovascular disorders.

Based on this, the aim of the present study was to investigate the relationship between obesity and cardiovascular damage, as well as to assess the effect of antioxidant administration in a fructose-induced experimental model. A deeper understanding of this relationship may contribute to the development of novel therapeutic strategies and prevention programs to combat this disease, which is reaching pandemic proportions and directly and indirectly impacts healthcare costs and the life expectancy of affected individuals.

II. AIM AND OBJECTIVES OF THE DISSERTATION

Aim:

To investigate the relationship between obesity and cardiovascular damage, as well as to assess the effect of antioxidant administration in a fructose-induced experimental model.

Objectives:

1. To investigate the metabolic changes and biochemical disturbances under a high-fructose diet (HFD).

2. To investigate the pathomorphological changes in cardiomyocytes, endothelial cells of the coronary vessels, and interlobar branches of the renal artery under a high-fructose diet (HFD).

3. To examine the role of oxidative stress and chronic low-grade inflammation in the development of cardiovascular damage under a high-fructose diet.

4. To investigate the role of SOD-1, NOS3, VCAM, and RIP3 in the development of cardiovascular damage under a high-fructose diet.

5. To assess the correlation between certain biomarkers of oxidative stress, metabolic disturbances, chronic low-grade inflammation, and the pathomorphological changes in cardiomyocytes, endothelial cells of the coronary vessels, and interlobar branches of the renal artery under a high-fructose diet.

6. To investigate the cardioprotective and vasculoprotective effects of S-AMe.

III MATERIALS AND METHODS

1. Main Procedures in In Vivo Experiments

1.1. Experimental animals

To establish our experimental model of obesity, 18 male Wistar rats weighing 120–160 g were used. The experimental animals were provided and bred by the central vivarium of the Medical University of Varna under standard laboratory conditions: a 12:12 h light-dark cycle, 50–60% humidity, temperature 22 ± 2ºC, with ad libitum access to food and water.

All procedures for conducting the experiment and treating the laboratory animals were carried out in compliance with the requirements of the Ethics Committee for Experimental Animals at the Bulgarian Food Safety Agency (BFSA), permit number 272/20.07.2020, as well as national regulations for working with experimental animals and the European Parliament Directive on the protection of animals used for scientific purposes (Directive 2010/63/EU of the European Parliament and of the Council of 22 September 2010).

The food provided during the study period was standard, prepared according to the manufacturer's recipe (HL-Top Mix Ltd.) with the following composition: crude protein – 20.08%; crude fat – 2.15%; crude fiber – 5.99%; crude ash – 5.26%; calcium – 0.72%; phosphorus – 0.59%; digestible phosphorus – 0.15%; sodium – 0.13%; lysine – 0.91%; methionine – 0.35%. The composition of the dietary supplements included vitamins, provitamins, and substances with similar effects: vitamin A – 4,500 IU/kg; vitamin D – 1,350 IU/kg; vitamin E – 13.5 IU/kg. Trace element mixtures contained: iron – 176.89 mg/kg; manganese – 91.87 mg/kg; zinc – 94.68 mg/kg; copper – 22.87 mg/kg; iodine – 0.92 mg/kg; selenium – 0.47 mg/kg.

1.2. Dietary Supplements and Other Substances Used

- *S-Adenosylmethionine (SAM)*

For a period of 12 weeks, the designated experimental animals received S-adenosylmethionine (SAM) in liquid form, administered orally (per os).

- *Glucose-Fructose Syrup*

To induce an experimental model of obesity, the designated treatment groups were given free access to a 20% glucose-fructose syrup solution for a period of 12 weeks. This solution was prepared from 52% fructose derived from corn syrup. The high-fructose corn syrup was certified for use as a sweetener and preservative in the food industry, produced by Amilum Factory – Razgrad (ISOGLUCOSE 031). According to the literature, an effective dose for implementing our experimental model was established (Meyers et al., 2017).

1.3 Experimental design

The experimental animals were divided into 3 groups (n = 6) based on the substances administered and the feeding regimen:

→ *First group – control (C)* – Rats subjected to a standard regimen with food and water

→ *Second group – Obesity model group (FRU)* – rats subjected to a high-fructose diet

→ *Third group – Obesity model group (FRU+SAM)* – rats subjected to a high-fructose diet and treated with S-adenosylmethionine, administered in the drinking water at a dose of 1 g/kg body weight.

The experimental animals underwent a two-week acclimation period prior to the introduction of S-adenosylmethionine (SAM) and glucose-fructose syrup. During this time, the body weight of each rat was measured and recorded in a protocol notebook. After the acclimation period, the animals were maintained on a standard diet ad libitum throughout the day. Daily monitoring included the intake of food, water, glucose solution, and S-adenosylmethionine (SAM), as well as observation of the animals' general health. Following acclimation, the second and third groups were subjected to a 12-week exposure to a 20% fructose syrup, a period necessary for the development of our experimental obesity model (Bratoeva et al., 2013; Wali et al., 2023). During the same period, animals in the third group also received supplementation with S-adenosylmethionine.

To determine changes in biochemical parameters, venous blood was collected from the jugular vein of the rats under preliminary anesthesia with Ketamine at a dose of 15–25 mg/kg i.m. (Anaket, solution pro injectionibus, Richter Pharma AG, Austria). Under general anesthesia with Ketamine, zoometric parameters, body mass index (BMI), and Lee index were assessed for each experimental animal.

At the end of the experimental period, the animals were euthanized using a lethal dose of Ketamine (148 mg/kg) (Rebuelto et al., 2002). Subsequently, autopsy with evisceration was performed according to the method of Koptyaeva et al. (2018), including macroscopic evaluation of the internal organs and elastic and musculo-elastic vessels (coronary arteries and interlobar branches of the renal arteries), followed by tissue preparation for morphological, morphometric, and immunohistochemical analysis. For this purpose, part of the necropsy material was immediately stored at –70ºC, while the remaining tissue was fixed in 10% neutral buffered formalin.

2. Analytical Methods Used

2.1 Zoometric Measurements

→ *Body Mass* – The body weight of the experimental animals during the acclimation period and throughout the experiment was recorded once a week using a digital scale, and the values were documented in a protocol notebook.
→ *Weight of Internal Organs (pancreas, liver, heart, kidneys, and RPAT)* – The weight of the internal organs was recorded once after autopsy using a digital scale, and the values were documented in a protocol notebook.
→ *Abdominal Circumference* – The abdominal circumference was measured in centimeters at the widest part of the abdomen with the animal placed in a supine position.
→ *Chest Circumference* – The chest circumference was measured in centimeters at the widest part of the thorax with the animal placed in a supine position.
→ *Length (Nose-to-Anus Distance)* – The distance from the nose to the anal opening was measured using a millimeter ruler.
→ *Lee Index* – Changes in body weight and the degree of obesity during the experiment were assessed using the Lee index (an anthropometric method), calculated as the cube root of body weight (g) divided by the nose-to-anus length (cm).
→ *TyG Index* – Calculated as Ln [(fasting triglycerides (mmol/L) × 88.57) × (fasting glucose (mmol/L) × 18) / 2].

2.2 Biochemical and Clinical Laboratory Methods

- Determination of Urea, Creatinine, Uric Acid, Glucose, Total Protein, Albumin, Liver Enzymes, Total Cholesterol, Triglycerides, VLDL, and HDL – The levels of urea, creatinine, uric acid, glucose, total protein, albumin, liver enzymes (γ-GT, AST, ALT), and lipid profile (triglycerides, total cholesterol, VLDL, and HDL) in serum were determined according to standard procedures using an automatic analyzer OLIMPUS AU 640.

- Determination of Serum Electrolyte Levels (Potassium, Sodium, Chloride, Calcium, Phosphorus, and Magnesium) – Conducted according to standard procedures using an automatic analyzer OLIMPUS AU 640.

2.3 Immunological Methods

- ***Determination of Serum TNF-α Levels***

Serum TNF-α levels in all experimental animals were determined using the Enzyme-Linked Immunosorbent Assay (ELISA) method, employing a commercially available Rat TNF-α kit (Diaclone SAS, Gen-Probe) with a 96-well plate for ELISA reading. Quantitative measurement of TNF-α values was performed according to the manufacturer's protocol.

- ***Determination of Serum CRP Levels***

Serum CRP levels in all experimental animals were determined using the immunoturbidimetric method, following standard procedures with an automatic analyzer OLIMPUS AU 640.

- ***Determination of Serum vitamin D3 (25-OH) Levels***

Serum vitamin D3 levels were determined using chemiluminescence with an automatic analyzer Alinity.

2.4. Morphological Methods

- ***Macroscopic Examination***

The heart, kidneys, and RPAT of each experimental animal were dissected according to the method of Koptyaeva et al., after which they were examined for macroscopic changes and weighed using a digital scale. Following the macroscopic evaluation, the tissue samples were fixed in 10% neutral formalin for subsequent histological, morphometric, and immunohistochemical analyses.

- ***Histological Methods***

Sample Processing

The heart of each experimental animal was dissected according to the method of Koptyaeva et al., after which three transverse sections of the left ventricle (4 μm thick) were prepared – at the apex, mid-ventricle, and near the aortic valve. Following kidney dissection, three transverse sections of the renal parenchyma including the interlobar branches of the renal artery were prepared. After fixation in 10% neutral buffered formalin, the samples were processed in paraffin with a melting point of 52–54ºC and paraffin blocks were prepared. The sections were routinely stained with hematoxylin-eosin for morphological and morphometric evaluation of histological changes in the cardiac muscle and interlobar branches of the renal artery.

- ***Morphometric Analysis of the Left Ventricle and Interlobar Branches of the Renal Artery***

For the morphometric analysis of the left ventricle, the wall thickness (in μm) was measured at three different locations – at the apex, mid-ventricle, and near the aortic valve. Therefore, three separate sections from the left ventricle of each experimental animal were prepared and examined at 40× magnification. For the morphometric analysis of the interlobar branches of the renal artery,

the internal diameter (μm), external diameter (μm), and the ratio of media thickness to internal diameter (μm) were measured. At least three measurements were taken from each section, and the values were recorded in a laboratory notebook and statistically processed. The morphometric analysis and the digital images of the scanned histological sections were performed using Aperio Image Scope V12.4.6.5003.

- ***Immunohistochemical Methods***

For the purposes of our immunohistochemical analysis, the immunoperoxidase method was used for sample preparation (EnVision™ FLEX, High-pH, DAKO, catalog number). The immunohistochemical staining procedure included the use of a peroxidase blocking reagent, a secondary antibody conjugated with the HRP enzyme, a chromogenic substrate diaminobenzidine (DAB), and hematoxylin for counterstaining. The expression of SOD-1, NOS3, RIP3, and VCAM was determined using the following polyclonal and monoclonal antibodies:

(1) SOD-1 antibody, Bio Vision Inc., USA, catalog number 3458-100, Lot #70658, polyclonal rabbit antibody, diluted 1:200
(2) NOS3 antibody, Santa Cruz Biotechnology, Inc., Germany, catalog number sc-376751, Lot #70658, monoclonal mouse antibody, diluted 1:300
(3) RIP3 antibody, Santa Cruz Biotechnology, Inc., Germany, catalog number sc-374639, Lot #D1521, diluted 1:400
(4) VCAM antibody, Santa Cruz Biotechnology, Inc., Germany, catalog number sc-13160, Lot #A2721, diluted 1:400

The specimens used for immunohistochemical analysis consisted of various sections of cardiac muscle and fragments of coronary and renal vessels. The collected material was fixed by immersion for 48 hours at room temperature in 10% neutral buffered formalin, and after dehydration through an ascending alcohol series, it was embedded in paraffin.
From the cardiac muscle and renal parenchyma, 4 μm-thick paraffin sections were prepared, mounted on silanized glass slides (Thermo Fisher Scientific), and dried for 24 hours at 37 ºC. After drying, the sections were deparaffinized at room temperature in two changes of xylene for 10 minutes each, followed by rehydration through a descending alcohol series: 100% ethanol for 5 minutes → 90% ethanol for 5 minutes → 80% ethanol for 5 minutes → 70% ethanol for 5 minutes. Finally, the sections were washed in running water and placed in dH_2O.

Immunohistochemical Protocol for Detection of SOD-1, NOS3, RIP3, and VCAM Expression

- Deparaffinization to dH_2O
- Antigen retrieval in antigen retrieval solution (DAKO) – high pH (pH 9.0) at 97 °C for 20 minutes, followed by cooling to 65 °C in PT Link (DAKO).
- Washing with wash buffer (TBS).
- Incubation with the primary antibody at the appropriate dilution at room temperature.

- Washing with wash buffer (TBS).
- Incubation with HRP-labeled polymer (goat anti-mouse, anti-rabbit) for 30 min at room temperature (1:100).
- Washing with washing buffer (TBS).
- Incubation of the sections with chromogen (diluted 1:20 in DAB) for 2 × 5 min with continuous microscopic monitoring.
- Rinse with distilled water (dH_2O).
- Counterstaining with hematoxylin
- Rinsing the samples with distilled water (dH_2O)
- Dehydration in an ascending ethanol series: 70% ethanol for 5 min → 80% ethanol for 5 min → 90% ethanol for 5 min → 100% ethanol for 5 min. Preparation of sections for mounting
- Mounting the sections using a coverslip (Thermo Fischer Scientific)

Using the Leica Aperio Scan Scope AT2 device, the sections were scanned and the images were analyzed with Aperio Image Scope software V12.4.6.5003. The intensity of the immune reaction in cardiomyocytes, coronary, and renal endothelial cells was assessed using a saturation index. Depending on the amount of deposited immune precipitate in individual cells, they were categorized into four grades (Detre et al., 1995):

- No precipitate – score 0
- Weak immune reaction – score 1
- Moderate immune reaction – score 2
- Strong immune reaction – score 3

The analysis was performed on a defined number of cells (cardiomyocytes, coronary, and renal endothelial cells). The mean intensity of the immune reaction was calculated by multiplying the number of cells in each category by the corresponding score (0, 1, 2, or 3), and then dividing the resulting sum by the total number of cells.

3. Statistical Analysis of Study Results

To achieve the objectives and address the tasks of our study, the following methods were employed:

- **Descriptive Methods**

A descriptive analysis was used to characterize the main features of the sample and the variables included in the study. Measures of central tendency, such as the arithmetic mean, were employed, along with non-parametric tests, including cross-tabulation and the chi-square test, to examine associations among categorical variables. Statistical significance for the non-parametric tests was set at $p \leq 0.05$.

- **Analytical Methods**

1. A T-test was used to compare the mean values between two groups to evaluate the effect of the drugs on treated and healthy rats. Differences between groups were considered statistically significant at $p \leq 0.05$.
2. Analysis of Variance (ANOVA) was used to compare the differences in treatment among the three experimental groups of treated rats. Differences were considered significant at $p < 0.05$, which is the accepted threshold for biological experiments.
3. Correlation analysis was applied to examine the relationships between variables and to determine the strength of their influence on tissue damage. The strength of the relationship between variables was assessed using Pearson's correlation coefficient (r). The degree of association between variables was classified as:

- Moderate: $0.5 < r \leq 0.7$
- Strong: $0.7 < r \leq 0.9$
- Very strong: $r > 0.9$
- Statistical significance was set at $p \leq 0.05$.

Statistical analysis was performed using SPSS v21, and graphs were created using GraphPad Prism 5.0.

IV. RESULTS AND DISCUSSION

1. Investigation of metabolic disorders associated with a High-Fructose Diet (HFD) and S-Adenosylmethionine (SAM) administration

1.1. Changes in zoometric parameters and weight of retroperitoneal adipose tissue

1.1.1 Results

- ***Results Obtained from the Measurement of Body Mass***

The body weight of the experimental animals from all groups was recorded weekly over a period of three months. Monitoring of body weight changes revealed a uniform increase in body mass values in all three groups until the end of the experiment. Table 1 presents the baseline body weight of the experimental animals, as well as the changes recorded in the 5th week, 9th week, and at the end of the experiment.

Table 1. Changes in Body Mass Over Time.

Period of Body Mass Measurement	C	F	F+S-AMe
Initial Body Weight	141,5 ± 6.8	136.8± 4.3	126.2± 3,8
5-th week	177.0± 9.8	181.3±9,8 *	151.8± 4.2
9-th week	231.2±14.5	231.0±12.4*	202.2±2.9
Final Body Weight /12-th week	265.5±12.89	268.8±16.0*	245.0±6.8

*Legend: Data are presented as mean ± standard error of the mean (SEM) (N = 6). C-control group; F-group on HFD; F+S-AMe- group on HFD and S-adenosine methionine supplementation; * p<0,05– Statistical significance between the F group and the F + S-AMe group.*

At the end of the experiment, rats in the fructose group showed a statistically significant increase in body weight compared to the control group at weeks 5, 9, and 12 ($p < 0.05$). In contrast, rats in the group treated with fructose and S-adenosylmethionine exhibited a statistically significant

reduction in body weight gain compared to the fructose group.

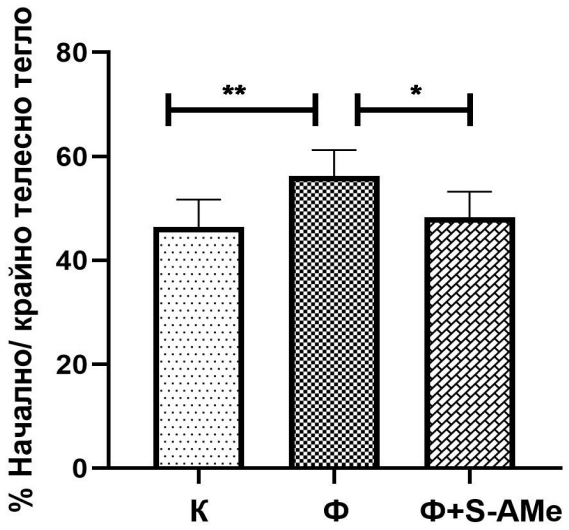

Fig.2. Changes in body weight gain among the experimental groups, Measured as a percentage of the animals' initial and final body weight.
*Legend: Data are presented as mean ± standard error of the mean (SEM) (n = 6). К – control group; Ф – high-fructose diet (HFD) group; Ф + S-AMe – HFD group supplemented with S-adenosylmethionine; *p < 0.05, p < 0.001, t-test.*

In Figure 2, we compared body weight gain among the different experimental groups, expressed as a percentage of the initial and final body weight. Supplementation of the experimental animals with S-AMe resulted in a statistically significant reduction in body weight compared to the fructose group ($p < 0.05$). Nevertheless, the high-fructose diet (HFD) group showed a statistically more significant increase in body weight compared to the control group ($p < 0.001$) (Figure 2)

- ***Results Obtained from Measurements of Length (Nose-to-Anus Distance), Abdominal Circumference, and Chest Circumference***

After measuring the nose-to-anus length (NAL), abdominal circumference (AC), and chest circumference (CC), we observed a statistically non-significant increase in these values in both the control and fructose groups. Administration of exogenous S-AMe to animals on a high-fructose diet (HFD) resulted in a slight reduction of the zoometric parameters compared to the fructose group (Table 2).

Table 2. Changes in Zoometric Parameters of Rats According to Experimental Group.

Zoometric parameter	C	F	F+S-AMe
NAL	23.08 ± 0.66	22.42 ± 0.31	22.75 ± 0.34
AC	16.45 ± 0.63	17.08 ± 0.48	16.57 ± 0.36
CC	15.00± 0.5	15.50 ± 0.4	14.77 ± 0.35

Legend: Data are presented as mean ± standard error of the mean (SEM) (N = 6). C – control group; F – high-fructose diet (HFD) group; F + S-AMe – HFD group receiving S-adenosylmethionine; NAL – nose-to-anus length; AC – abdominal circumference; CC – chest circumference."

- ***Results obtained from calculating the Lee index***

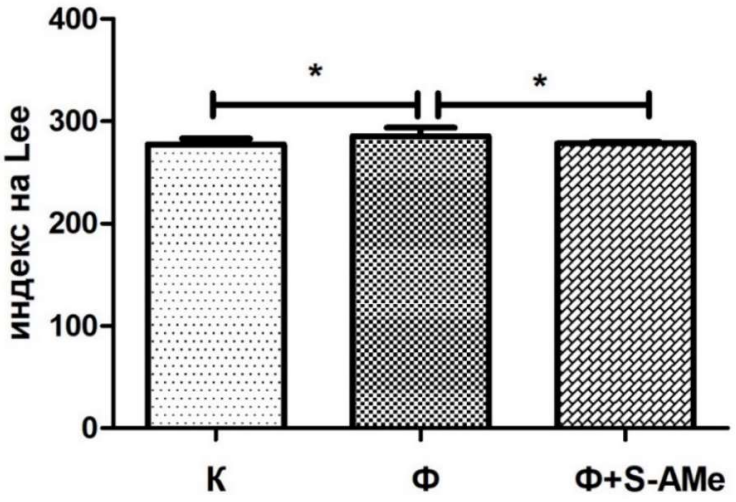

Fig. 3 Differences in the Lee index among animals in the experimental groups. Legend: Data are presented as mean ± standard error of the mean (SEM) (N = 6). К – control group; Ф – high-fructose diet (HFD) group; Ф + S-AMe – HFD group receiving S-adenosylmethionine; p < 0.05, t-test

The results of our study indicate a trend toward a statistically significant increase in the Lee Index in animals from the fructose group compared to the control group ($p < 0.05$). In rats on a high-fructose diet (HFD) supplemented with S-AMe, a decrease in the Lee Index was observed compared to the fructose group, which was statistically significant ($p < 0.05$). Following S-AMe supplementation, the Lee Index values approached those of the control group (Fig.3).

- ***Results obtained from measurements of Retroperitoneal adipose tissue weight and Heart weight***

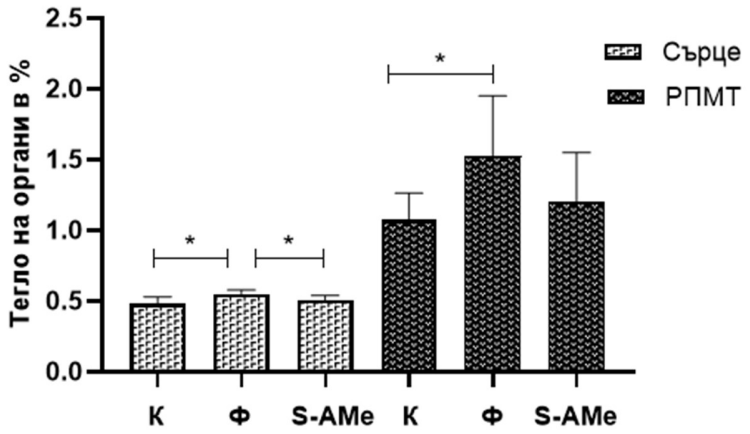

Fig. 4. Weight of Retroperitoneal Adipose Tissue and Heart, expressed as a percentage of total body weight of rats. Data are presented as mean ± standard error of the mean (SEM) (N = 6).
Legend: К – control group; Ф – high-fructose diet (HFD) group; Ф + S-AMe – HFD group receiving S-adenosylmethionine; $p < 0.05$

The results of the analysis of visceral adipose tissue weight, measured as a percentage of total body weight of the experimental animals, showed a statistically significant difference between rats in the fructose group and the control group ($p < 0.05$); animals in the fructose group exhibited an increase in retroperitoneal adipose tissue (RPAT) weight compared to controls. Supplementation with exogenous S-AMe resulted in a statistically non-significant reduction in visceral adipose tissue compared to HFD animals. Analysis of heart weight revealed a statistically significant increase in the fructose group compared to controls ($p < 0.05$), while S-AMe supplementation led to a statistically significant decrease in heart weight compared to the fructose group (Figure 4).

1.1.2 Discussion

For the implementation of our experiment, male Wistar rats were subjected to a high-fructose diet (HFD). We observed that, despite no differences in total caloric intake among the experimental animals, rats fed with fructose exhibited changes in zoometric parameters and an increase in body weight compared to the control animals at the end of the experiment (Table 1). It is important to note that excessive fructose consumption in the modern diet represents a major etiological factor in the development of metabolic disorders, as its intake is associated with visceral obesity and related cardiometabolic disturbances. Various pathogenic mechanisms explain the development of fructose-induced visceral obesity. High fructose consumption affects the central nervous system,

influencing the centers regulating hunger and satiety. HFD-fed rodents also demonstrate higher ghrelin levels and lower leptin levels compared to animals on a standard diet (Lindqvist et al., 2008), leading to hyperphagia, increased energy intake, and triglyceride accumulation in adipocytes with subsequent weight gain. This is also demonstrated in our experimental model of fructose-induced obesity, in which a statistically significant increase in retroperitoneal adipose tissue (RPAT) weight was observed compared to the control group, a hallmark of visceral-type obesity (Figure 4). These results are consistent with the findings of Tan et al., who reported that triglycerides begin to accumulate ectopically in various organs, such as visceral adipose tissue (VAT), liver, and skeletal muscle, once the storage capacity of adipocytes is exceeded (Tan et al., 2008). It has also been demonstrated that fructose-induced adipogenesis is mediated by elevated levels of 11β-hydroxysteroid dehydrogenase type 1 (11β-HSD1) in VAT, which increases glucocorticoid production and, consequently, fat accumulation in the retroperitoneal space (London E. et al., 2011). On the other hand, supplementation with S-AMe resulted in a significant reduction in RPAT weight, approaching that of the control group.

In addition to RPAT weight, the results obtained from the measurement of zoometric parameters, namely abdominal circumference (AC) and chest circumference (CC), were also significant in our experiment. A statistically non-significant increase in AC and CC was observed in the fructose group compared to the control group and the groups supplemented with SAM (Table 2). These findings support the claim of some authors (Esfandiari et al., 2007) that exogenous SAM administration suppresses lipogenesis, leading to reductions in AC, CC, and body weight. Another possible mechanism linking SAM supplementation to decreased body weight and zoometric parameters is the inhibition of leptin secretion, resulting in reduced food intake and enhanced satiety (Lu SC et al., 2012). In contrast to our results, other authors (Martínez-Uña et al., 2013; Elshorbagy AK et al., 2013) have demonstrated that high serum levels of SAM can promote visceral obesity and the development of hepatic steatosis.

Several decades ago, Lee (1929) developed an index to classify obesity in rats with similar BMI, which was later also applied for the same purpose in humans. The Lee Index positively correlates with body weight and body fat percentage in experimental animals subjected to fructose-induced obesity, making it a reliable predictor of obesity in rodents (Molz et al., 2017). Our results demonstrate an increase in the Lee Index in the fructose group, which was statistically significant (Figure 3). This supports the claim of some authors that values close to or exceeding 300 are widely accepted as indicators of obesity in rats (Simson et al., 1982). On the other hand, rats on a high-fructose diet (HFD) supplemented with the antioxidant S-AMe exhibited body weight loss and a reduction in the Lee Index to values approaching those of the control group. This confirms the findings of Esfandiari et al. (2007), who reported that S-AMe effectively suppresses lipogenesis, reduces total body fat percentage, and decreases visceral adipose tissue. Other mechanisms explaining the anti-obesogenic activity of S-AMe include reactive oxygen species (ROS) scavenging, inhibition of lipid peroxidation (reduced MDA levels), and enhancement of endogenous antioxidants (Cavallaro et al., 2010).

It is well established that visceral obesity represents a significant risk factor for cardiovascular disease, as it leads to vascular inflammation, endothelial dysfunction, vascular remodeling, and

oxidative stress. Therefore, at the conclusion of our experiment, we can state that administration of the antioxidant S-AMe significantly attenuates the development of various cardiometabolic disturbances by reducing body weight, RPAT weight, and anthropometric measurements.

1.2. Variations in Lipid and Carbohydrate Metabolism

1.2.1 Results obtained from the assessment of serum glucose, serum lipids, and the TyG index

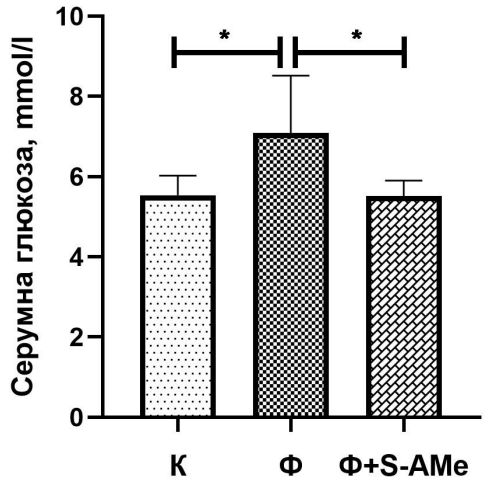

Fig. 5. Changes in Serum Glucose Levels in the Experimental Groups.
Legend: Data are presented as mean ± standard error of the mean (SEM) (n = 6). К – control group; Ф – high-fructose diet (HFD) group; Ф + S-AMe – HFD group supplemented with S-adenosylmethionine; p < 0.05, t-test."

Analysis of the biochemical assessment of serum glucose revealed statistically significantly higher values in the fructose group compared to the control group ($p < 0.05$). A statistically significant difference was also observed between the fructose group and the HFD group supplemented with S-AMe ($p < 0.05$) (Figure 5).

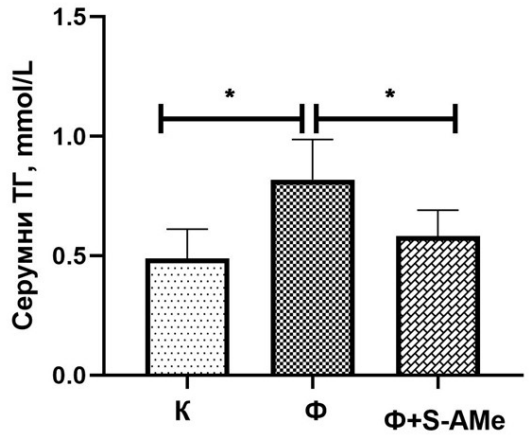

Fig. 6. Changes in Serum Triglyceride (TG) Levels in the Experimental Groups.
Legend: Data are presented as mean ± standard error of the mean (SEM) (n = 6). К – control group; Ф – high-fructose diet (HFD) group; FФ+ S-AMe – HFD group supplemented with S-adenosylmethionine; p < 0.05, t-test

In Figure 6, statistically significantly higher serum triglyceride (TG) levels were observed in the fructose group compared to the control group ($p < 0.05$). Administration of S-AMe in the HFD group reduced serum TG levels, bringing them closer to control values, which was also statistically significant ($p < 0.05$).

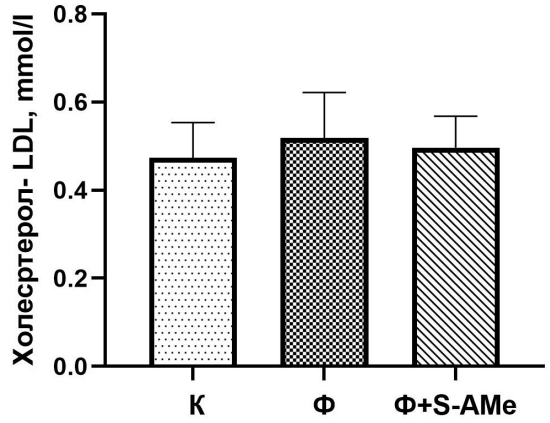

Fig. 7. Changes in Serum LDL Levels in the Experimental Groups.
Legend: Data are presented as mean ± standard error of the mean (SEM) (n = 6). К – control group; Ф – high-fructose diet (HFD) group; Ф + S-AMe – HFD group supplemented with S-adenosylmethionine.

The results of the biochemical assessment show a trend toward increased serum LDL levels in the fructose group compared to the control group, although this was not statistically significant. In HFD animals supplemented with S-AMe, a slight decrease in LDL levels was observed, bringing

them closer to those of the control group, but this change was also not statistically significant (Figure 7).

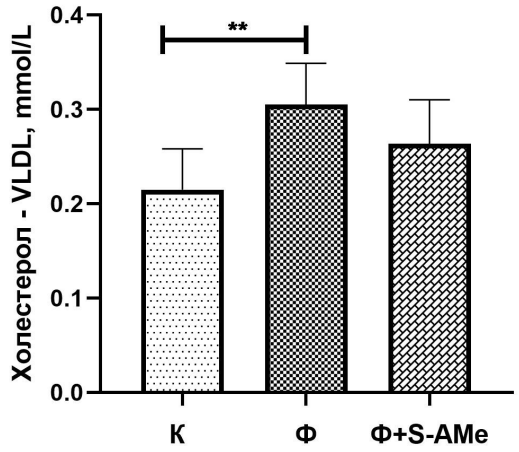

Fig. 8. Changes in Serum VLDL Levels in the Experimental Groups.
Legend: Data are presented as mean ± standard error of the mean (SEM) (n = 6). К – control group; Ф – high-fructose diet (HFD) group; Ф + S-AMe – HFD group supplemented with S-adenosylmethionine; p < 0.01, t-test.

Our results show statistically significantly higher VLDL levels in the fructose group compared to the control group ($p < 0.01$). In contrast, in the HFD group supplemented with S-AMe, a decrease in VLDL levels was observed compared to the fructose group (Figure 8).

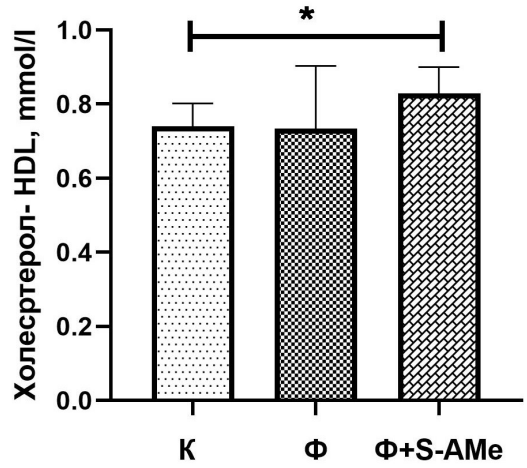

Fig. 9. Changes in Serum HDL Levels in the Experimental Groups.
Legend: Data are presented as mean ± standard error of the mean (SEM) (n = 6). К – control group; Ф – high-fructose diet (HFD) group; Ф + S-AMe – HFD group supplemented with S-adenosylmethionine; p < 0.05, t-test.

HDL levels were significantly increased in the group supplemented with S-AMe compared to the control group ($p < 0.05$). No statistically significant differences in HDL levels were observed between the control and fructose groups (Figure 9).

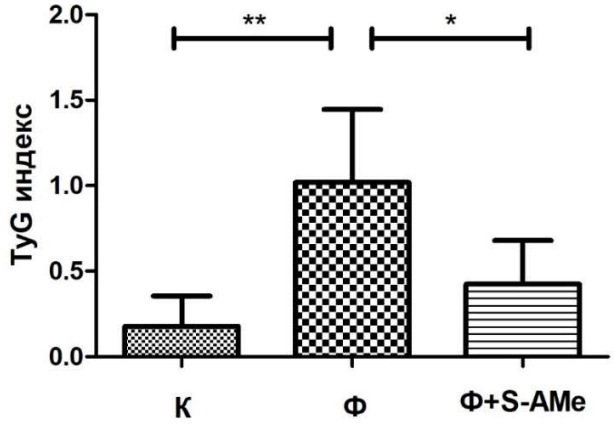

Fig. 10. Changes in the TyG Index in the Experimental Groups.
*Legend: Data are presented as mean ± standard error of the mean (SEM) (n = 6). К – control group; Ф – high-fructose diet (HFD) group; Ф + S-AMe – HFD group supplemented with S-adenosylmethionine; *p < 0.05, p < 0.01, t-test.*

TyG index values (triglyceride/glucose ratio) were significantly increased in the HFD group compared to the control group ($p < 0.01$). In the group supplemented with S-AMe, TyG index values were significantly lower compared to the fructose group ($p < 0.05$) (Figure 10).

1.2.2 Discussion

Mechanisms of Fructose-Induced Hyperlipidemia

Various studies have confirmed the association between excessive fructose intake and the development of conditions such as metabolic syndrome, dyslipidemia, metabolic dysfunction-associated steatotic liver disease (MASLD), and obesity (Hieronimus et al., 2020; Regnault et al., 2013, et al.). High consumption of foods and beverages sweetened with HFCS significantly contributes to the rising prevalence of obesity-related metabolic disturbances, including hyperglycemia and type 2 diabetes (Wang M. et al., 2015; Malik V. S. et al., 2010).

These changes were also observed in our experimental animals. At the end of the study, higher levels of TG, VLDL, and LDL were detected in the fructose group compared to the control group, with the increases in TG and VLDL being statistically significant, while LDL showed only a trend toward elevation. On the other hand, SAM supplementation had a beneficial effect on lipid metabolism by significantly reducing TG levels, bringing them closer to control values,

and lowering VLDL and LDL levels (Figures 6, 7, 8). A slight decrease in serum HDL levels was observed in the fructose group compared to the control group, whereas the supplemented animals demonstrated statistically significantly higher HDL levels compared to controls (Figures 9, 11).

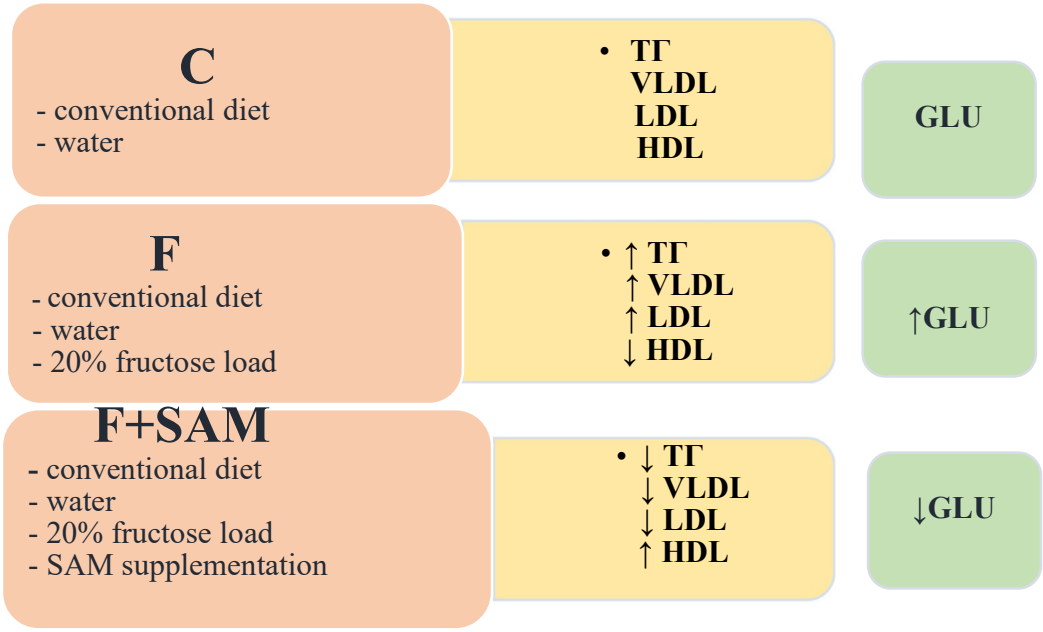

Fig. 11. Changes in Lipid Parameters and Serum Glucose Following Fructose Load and SAM Administration. Legend: C – control; Fru – HFD group; Fru + SAM – HFD group supplemented with SAM; TG – triglycerides; VLDL – very low-density lipoproteins; LDL – low-density lipoproteins; HDL – high-density lipoproteins; GLU – glucose.

Our results confirm the observations of other authors (Girard et al., 2006) regarding the pathogenetic link between fructose consumption and the development of hypertriglyceridemia and hypercholesterolemia. Several mechanisms explain this association, including increased de novo lipogenesis, elevated production and impaired catabolism of VLDL, and reduced TG clearance due to decreased lipoprotein lipase activity (Girard et al., 2006). Another possible mechanism is fructose-induced impairment of β-oxidation, resulting from increased de novo lipogenesis with subsequent accumulation of malonyl-CoA, which acts as an allosteric inhibitor of CPT1α, thereby disrupting fatty acid translocation into mitochondria and redirecting them toward TG, LDL, and VLDL synthesis. According to Aeberli et al., fructose increases small dense LDL particles, which are associated with a higher risk of atherosclerosis (Aeberli I., et al., 2011). Conversely, other authors report that HFCS consumption as part of an eucaloric diet for 10 weeks does not adversely affect the lipid profile in overweight or obese individuals (Lowndes J., et al., 2014). Based on current evidence, it appears that the intake of moderate amounts of

fructose (<50 g/day) alone does not lead to an unfavorable lipid profile (Sievenpiper J. L., et al., 2014).

According to Chong et al., fructose is rapidly incorporated into both glycerol and fatty acyl-CoA, which are key components of triglycerides (Chong et al., 2007), thereby acting as a driver in the progression of hypertriglyceridemia, elevated VLDL levels, de novo lipogenesis, and eventually the development of NAFLD. It has also been shown that fructose stimulates sterol regulatory element-binding protein 1 (SREBP-1c) and carbohydrate-responsive element-binding protein (ChREBP), both of which are key transcriptional regulators of hepatic de novo lipogenesis (Hannou S.A. et al., 2018). In addition to the role of ChREBP in fructose-induced dyslipidemia, Erion et al. demonstrated that ChREBP "knockout" enhances peripheral insulin sensitivity in HFD-fed rats (Erion DM. et al., 2013) (Figure 13).

The exact mechanisms by which SAM reduces serum lipid levels remain unclear. According to a study by Vergani L. et al. on steatotic FaO rat hepatoma cell lines, SAM administration led to a several-fold increase in CTP1 mRNA expression, promoting mitochondrial fatty acid influx and stimulating β-oxidation (Vergani L. et al., 2020). Furthermore, SAM supplementation suppresses catalase activity, a key enzyme in the pathogenesis of oxidative stress, which drives reactive oxygen species (ROS) production and lipid peroxidation (Vergani L. et al., 2020). The antioxidant activity of SAM directly reduces cardiovascular risk through its protective effect on dysfunctional adipose tissue, which is characterized by elevated circulating levels of C-reactive protein, TNF-α, MCP-1, IL-6, procoagulants, ROS, and other factors that induce chronic nonspecific inflammation, endothelial dysfunction, oxidative stress, and insulin resistance.

Traditional diagnostic criteria for metabolic syndrome require a panel of laboratory tests and clinical assessments, which often limits their widespread application in screening programs (Grundy S.M. et al., 2005). Early detection of metabolic syndrome is crucial for implementing measures to prevent subsequent obesity-related cardiometabolic disorders and cardiovascular damage. Consequently, current clinical practice has shown increasing interest in certain anthropometabolic indices that combine anthropometric measurements (such as body weight, height, and waist circumference) with key metabolic parameters (such as serum glucose and triglycerides) to identify the risk of metabolic syndrome (Liu X.C. et al., 2021).

In our experimental model, we observed a significant increase in the triglyceride-glucose index (TyG)—the ratio of serum triglycerides to glucose—in the HFD group compared to the control group (Figure 10). Numerous studies have shown that the TyG index serves as an effective tool for clinically predicting metabolic syndrome, as it reflects pancreatic function and tissue insulin resistance (Ramdas Nayak V.K. et al., 2022). Insulin resistance (IR) plays a critical role in the development of prediabetic conditions, including impaired glucose tolerance, diabetes mellitus (DM), and cardiovascular disease (CVD). Therefore, the TyG index represents a reliable prognostic marker for disease outcomes in these patients (Hill M.A. et al., 2021). Some of the mechanisms underlying the link between IR and CVD are illustrated in Figure 12. Wan et al. report that the predictive performance of the TyG index exceeds that of existing surrogate indices, including the Homeostasis Model Assessment of Insulin Resistance (HOMA-IR) (Wan H. et al., 2024). Furthermore, additional indices combining the TyG index with anthropometric

parameters—such as waist circumference (TyG-WC), waist-to-height ratio (TyG-WHtR), and body mass index (TyG-BMI)—also demonstrate significant accuracy in assessing cardiometabolic risk (Zhang Q. et al., 2023).

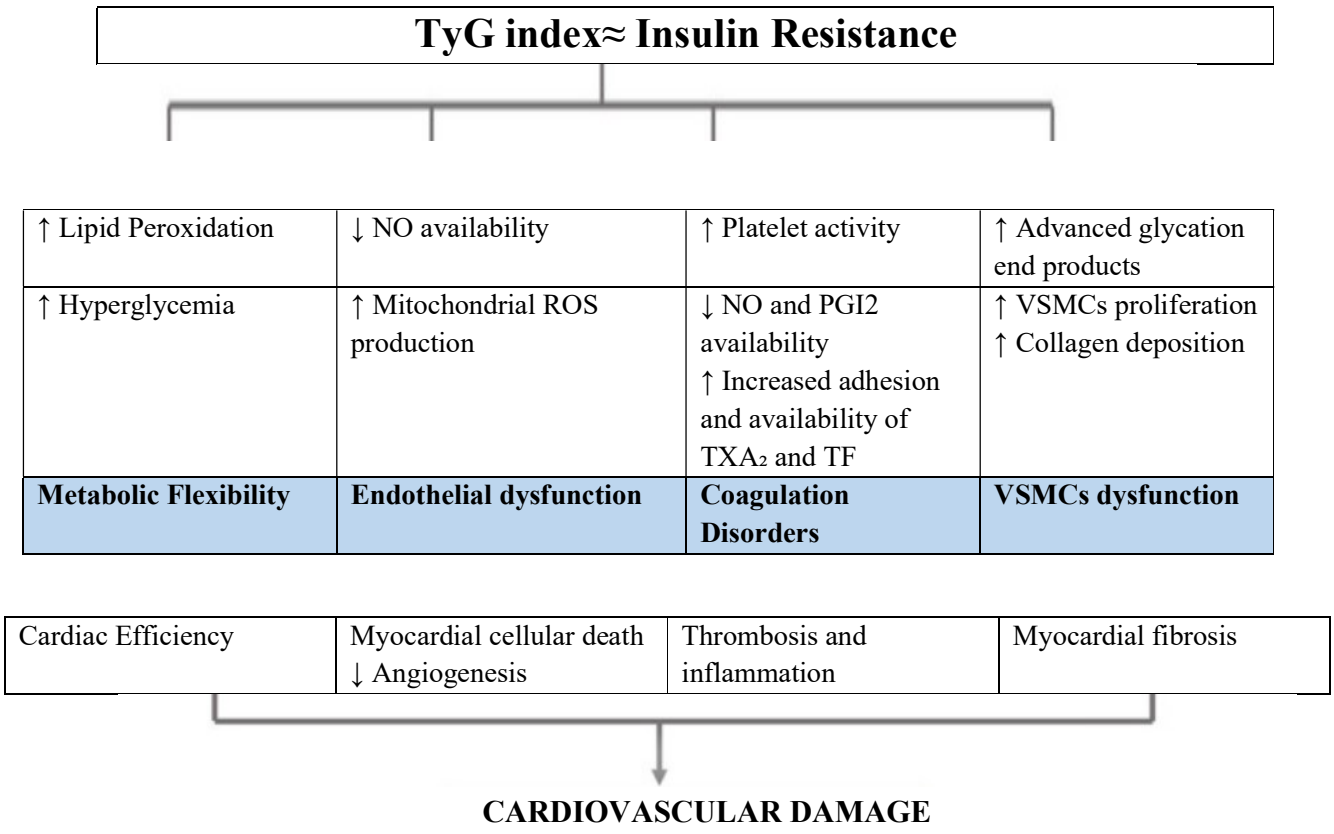

Fig. 12. Pathogenetic Mechanisms Contributing to the Predictive Value of the TyG Index for Cardiovascular Disease Outcomes.Legend: PGI_2 – prostacyclin; NO – nitric oxide; VSMCs – vascular smooth muscle cells; TXA_2 – thromboxane A_2; TF – tissue factor.

Despite its widespread use, the application of the TyG index as a marker for predicting cardiovascular risk remains associated with certain limitations. The original concept behind its introduction in 2008 was to demonstrate that insulin resistance is a key pathophysiological factor contributing to elevated serum triglyceride and glucose levels even in clinically healthy individuals (Simental-Mendía L.E. et al., 2008). The authors reported that TyG index values in patients with cardiovascular disease may be influenced by the dynamic changes in lipid and glucose profiles. This highlights the need for strict control of hyperglycemia and hyperlipidemia to ensure the validity of the TyG index as a predictive biomarker. In addition, some studies have not identified a significant association between the TyG index and the presence of cardiovascular disease; for example, Cho Y.R. et al. (2019) found no significant relationship in a cohort of 996 patients with diabetes after adjustment for classical cardiovascular risk factors. The relevance of the TyG index in our experimental model is supported by the observation that SAM supplementation resulted in a statistically significant reduction in its values compared to the

fructose group (Figure 10).
Despite the aforementioned limitations, the TyG index, as an indirect marker of insulin resistance, remains a reliable tool for identifying individuals at increased risk of developing diabetes mellitus. This makes it a valuable biomarker for both early detection and intervention, as well as for predicting outcomes in cardiovascular disease.

Mechanisms of Fructose-Induced Hyperglycemia and Insulin Resistance

In the context of carbohydrate metabolism, fructose is closely associated with progressive hyperglycemia and the development of type 2 diabetes mellitus. This is reflected in our biochemical analysis, which demonstrated a statistically significant increase in serum glucose levels in the HFD group compared to controls. In contrast, the SAM-supplemented group showed a statistically significant reduction in glucose levels compared to the fructose group, with values even lower than those observed in control animals (Figure 5). Several mechanisms underlie the development of fructose-induced hyperglycemia, including stimulation of gluconeogenesis and the development of insulin resistance, resulting in impaired glucose utilization in peripheral tissues.

Fructose is primarily metabolized in the liver into various substrates, including glucose, glycogen, lactate, and fatty acids. The first step of this process involves the rapid and uncontrolled conversion of fructose to fructose-1-phosphate (F1P) by fructokinase, a key insulin-independent enzyme, bypassing the central glycolytic regulatory control mediated by phosphofructokinase. This provides an uncontrolled flux of lipogenic substrates (acetyl-CoA and glycerol-3-phosphate) into alternative, insulin-independent pathways for triglyceride synthesis (Kolderup A. et al., 2015). This, in turn, leads to lipid accumulation in the liver, contributing to hepatic insulin resistance, and in the pancreas, impairing insulin synthesis and secretion (Sellami E. et al., 2023). Our results support the observations of other authors, showing that hepatic insulin signaling decreases in rodents exposed to HFD for 28 days (Ueno et al., 2000).

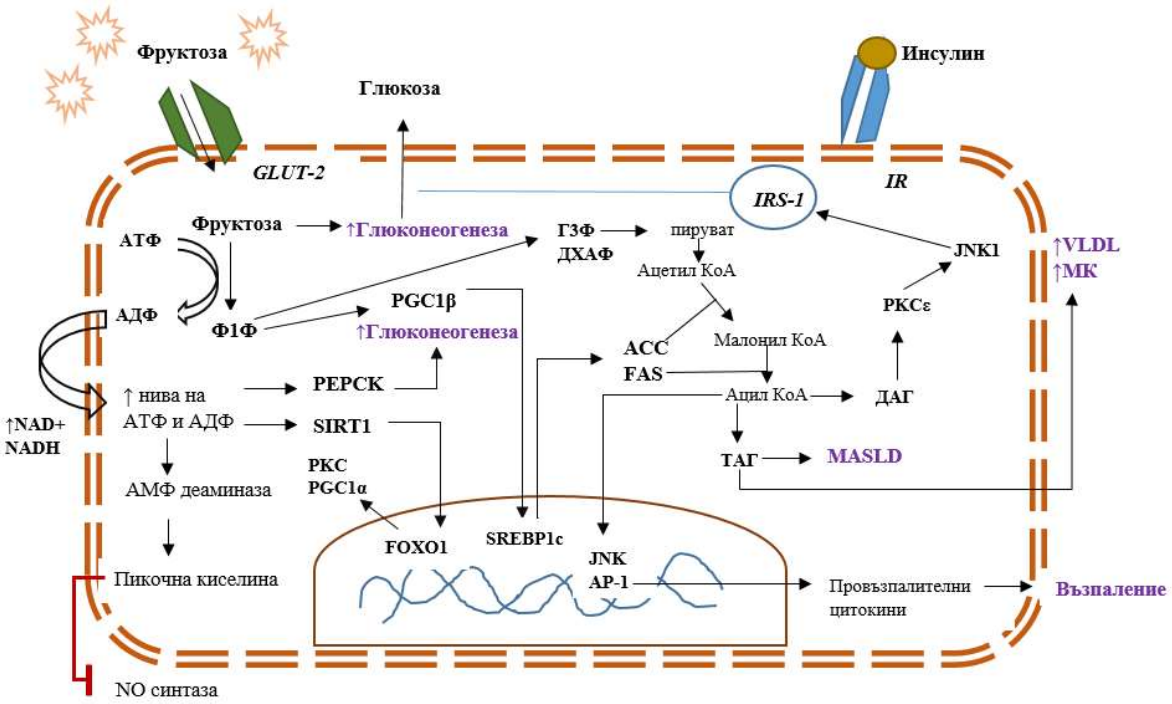

Fig. 13. Mechanisms of Fructose-Induced Hyperglycemia.
Legend: GLUT-2 – glucose transporter 2; F1P – fructose-1-phosphate; ATP – adenosine triphosphate; АТФ – adenosine diphosphate; PEPCK – phosphoenolpyruvate carboxykinase; SIRT1 – sirtuin-1; FOXO1 – forkhead box protein O1; PGC1 – peroxisome proliferator-activated receptor gamma coactivator 1; SREBP1c – sterol regulatory element-binding protein 1c; FAS – fatty acid synthase; ACC – acetyl-CoA carboxylase; IR – insulin receptor; ГЗФ – glyceraldehyde-3-phosphate; ДХАФ – dihydroxyacetone phosphate; JNK – c-Jun N-terminal kinase 1; AP-1 – activator protein 1; ДАГ – diacylglycerol; ТАГ – triacylglycerol; MASLD – metabolic dysfunction-associated steatotic liver disease.

The conversion of fructose to F1P is a high-energy process that decreases cellular ATP levels and increases ADP and AMP content, thereby raising the NAD^+/NADH ratio (Figure 13). The increase in NAD^+/NADH is associated with enhanced SIRT-1 activity, which, through deacetylation of FoxO1, stimulates the expression of PKC and PGC1α (Caton et al., 2011; Frescas et al., 2005), leading to increased hepatic gluconeogenesis and the development of hyperglycemia. Fructose entry into the cell also activates other energy pathways affecting carbohydrate metabolism. Accumulation of fructose-1-phosphate provides substrates (glycerol-3-phosphate) for the Krebs cycle, leading to the formation of malonyl-CoA and acyl-CoA (Figure 13).

A portion of acyl-CoA is converted to DAG, which activates JNK1, resulting in phosphorylation of serine residues on IRS-1 (IRS-1Ser307) and the development of insulin resistance and hyperglycemia (Hirosumi et al., 2002). In addition to the development of IR, JNK also activates

the transcription factor AP-1, promoting the production of ROS and proinflammatory cytokines (Baffy et al., 2009) and inducing oxidative stress, which further impairs insulin signaling and disrupts peripheral glucose utilization. Supporting this, SAM administration, as a potent antioxidant, reduced serum glucose levels in the treated animals in our experimental model.

Under normal conditions, insulin secretion is associated with inhibition of lipolysis. In contrast, under insulin-resistant (IR) conditions, increased release of free fatty acids (FFAs) into the bloodstream occurs, which accumulate in skeletal muscle and liver, exert lipotoxic effects, and contribute to the development of insulin resistance (Sellami E. et al., 2023). Accumulation of FFAs in these organs disrupts cellular organelles, leading to the release of reactive oxygen species (ROS) and proinflammatory cytokines. This triggers chronic low-grade inflammation, which impairs insulin signaling (β-cell dysfunction), disrupts glucose homeostasis, and results in systemic metabolic dysregulation (Ahmed et al., 2021).Prolonged hyperglycemia also exhibits glucotoxicity, causing cellular exhaustion, altered intracellular energy metabolism, oxidative stress, mitochondrial dysfunction, and progressive, irreversible damage to pancreatic β-cells (Liu X. et al., 2024). Insulin resistance, in turn, alters lipid and carbohydrate metabolism, leading to elevated levels of glucose, triglycerides (TG), VLDL, and LDL, and reduced HDL levels. These changes, together with endothelial dysfunction caused by abnormal insulin signaling, contribute to atherogenic plaque formation and increased cardiovascular risk.

The precise mechanisms by which SAM administration improves glucose homeostasis are still not fully elucidated. Some studies reporting significant improvements in glucose metabolism following SAM treatment in diabetic models attribute these effects to enhanced insulin sensitivity and glucose uptake through phosphorylation of IRS-1 and Akt (Izu H. et al., 2019; Moon M.K. et al., 2010).

1.3. Variations in Serum Uric Acid Levels

1.3.1 Results from the Measurement of Serum Uric Acid

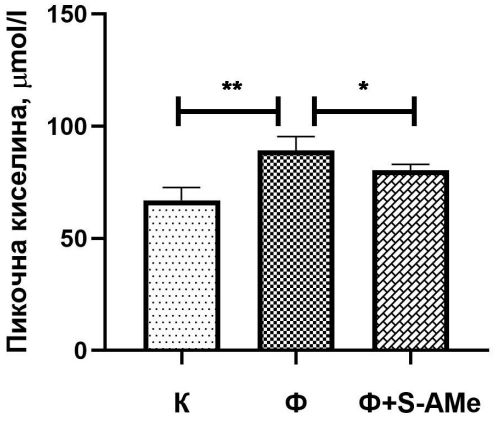

Fig. 14. Changes in Serum Uric Acid Levels in the Experimental Groups. Legend: Data are presented as

*mean ± standard error of the mean (SEM), (n=6). K – control group; Φ – HFD group; Φ+S-AMe – HFD group supplemented with S-adenosylmethionine; *p<0.05; p<0.01, t-test.*

The results of our study demonstrate an increase in serum uric acid levels in experimental rats subjected to HFD compared to the control group, which was statistically significant (*p<0.01). Administration of the antioxidant S-AMe led to a statistically significant reduction in uric acid levels compared to the fructose group (p<0.05) (Figure 14).

1.3.2 Discussion

Several studies have shown that the specific metabolism of fructose increases uric acid levels, which in turn affects the intensity of lipogenesis and contributes to the development of metabolic syndrome, insulin resistance, MASLD, leptin resistance, gout, and cardiovascular disease (Lubawy et al., 2023; Cicero et al., 2018). Our data demonstrate a statistically significant increase in uric acid levels in the HFD group compared to controls. Conversely, administration of SAM led to a statistically significant reduction in uric acid levels compared to the fructose group (Figure 14).

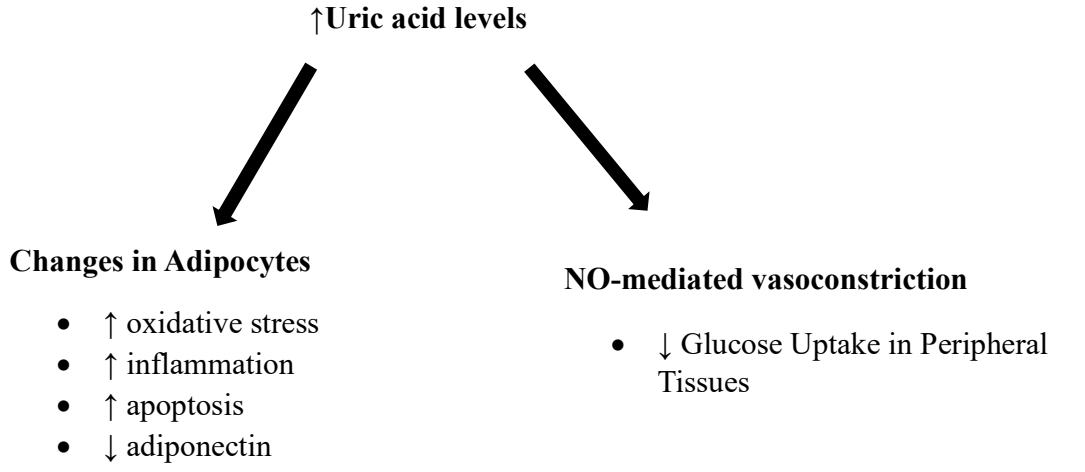

Fig. 15. Metabolic Changes Mediated by Uric Acid

Fructose phosphorylation, mediated by fructokinase, lacks a negative feedback mechanism, leading to rapid depletion of intracellular ATP, activation of AMP deaminase, and generation of uric acid, which induces cellular damage (Figure 15). Uric acid enters renal tubular cells, vascular smooth muscle, and adipocytes via the specific transporter URAT-1, activating NOX and resulting in reactive oxygen species (ROS) production and oxidative stress. Supporting this, our study demonstrated that SAM administration was associated with lower uric acid levels. According to Lanaspa et al. (2020), uric acid induces mitochondrial dysfunction and ROS

generation through NADPH oxidase activation and ATP depletion. Uric acid reduces endothelial NO levels by strongly inhibiting nitric oxide synthase (Gersch et al., 2008). NO plays a key role in endothelial function due to its vasodilatory effects. Consumption of an HFD, by increasing uric acid levels, adversely affects vascular regulation and elevates the risk of vascular inflammation, oxidative stress, atherosclerosis, and arterial hypertension (Russo et al., 2020; Nakagawa et al., 2005). Furthermore, Spiga et al. (2017) reported that uric acid activates the inflammatory NF-κB signaling pathway, increasing the expression of inflammatory biomarkers such as CRP, fibrinogen, ferritin, and complement C3 in hepatic G2 cells, thereby promoting inflammation, oxidative stress (Milanesi et al., 2019), and endothelial dysfunction. Consequently, uric acid plays a role in the development of insulin resistance and metabolic syndrome (Yu et al., 2010). Elevated uric acid levels contribute to a proinflammatory state by increasing MCP-1 synthesis and reducing adiponectin levels. The metabolic impact of uric acid is further supported by Umano et al. (2019), who found that lowering uric acid reduced macrophage infiltration and TNF-α expression, while improving insulin sensitivity and blood pressure in animal models. Taken together, these findings support the hypothesis that serum uric acid plays a key role in the pathogenesis of obesity and its associated complications.

1.4. Variations in serum Vitamin D3 (25-OH) levels and assessment of the correlation between vitamin D3 and the TyG index

1.4.1 Results

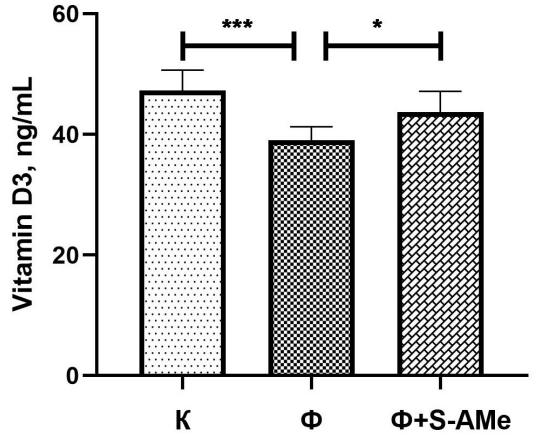

*Fig. 16. Changes in Serum Vitamin D3 (25-OH) Levels. Legend: Data are presented as mean ± standard error of the mean (SEM), (n=6). K – control group; F – HFD group; F+S-AMe – HFD group supplemented with S-adenosylmethionine; * p<0.05; *** p<0.001, t-test.*

Our results demonstrate a statistically significant decrease in serum Vitamin D3 (25-OH) levels in the fructose group compared to the control group (**p<0.001). In contrast, the group supplemented with the antioxidant S-AMe showed an increase in Vitamin D3 (25-OH) levels,

which was statistically significant ($p<0.05$) (Figure 16).

- ***Results obtained from the assessment of the correlation between Vitamin D3 and the TyG Index***

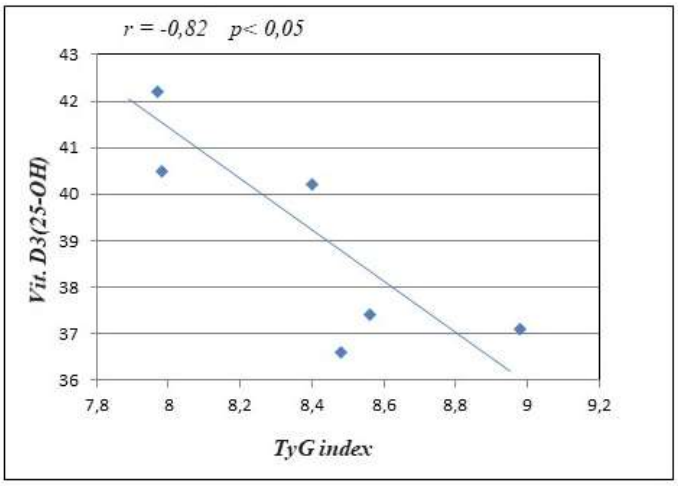

*Fig. 17. Correlation Between Serum Vitamin D3 Levels and the TyG Index in the HFD Group. Legend: Data are presented as mean ± standard error of the mean (SEM), (n=6). * p<0.05; ** r<-0.82, t-test.*

The results demonstrate a very strong negative correlation ($r = -0.82$; $p<0.05$) between the decrease in serum Vitamin D3 levels and the increase in the TyG index in the HFD group (Figure 17).

1.4.2 Discussion

The results of our study demonstrate that a high-fructose diet (HFD) induces a statistically significant reduction in serum Vitamin D3 (25-OH) levels in the Fructose group compared to the control group. In contrast, in the HFD group supplemented with SAM, an increase in Vitamin D3 (25-OH) levels was observed compared to the Fructose group, which was also statistically significant (Figure 16). We hypothesize that HFD leads to a decrease in Vitamin D3 (25-OH) through its effects on obesity development and associated oxidative stress, inflammation, and cellular damage. This is supported by a study by Derbel et al. (2025), which found that Vitamin D3 levels are significantly lower in obese individuals and positively correlate with BMI. This can partly be explained by the sedentary lifestyle often associated with these individuals. The hydrophobic nature of Vitamin D3 allows it to leave the circulation and accumulate substantially in adipose tissue in obese individuals, representing another potential mechanism underlying the inverse relationship between serum Vitamin D3 levels and BMI (Derbel et al., 2025; Alzohily et al., 2024).

This phenomenon was further demonstrated in studies by Mawer et al. (1972), who injected radiolabeled Vitamin D in patients and found that its highest activity levels were in adipose tissue. Conversely, Vitamin D deficiency may contribute to obesity development, as it plays a role in regulating lipogenesis and lipolysis (Mai et al., 2012). According to Fan et al., the transcription of the UCP3 gene is initiated by the binding of $1,25(OH)_2D_3$ (calcitriol)/VDR to the UCP3 promoter at the molecular level, enhancing energy metabolism and conferring resistance to diet-induced obesity (Fan et al., 2016). These findings highlight the existence of a vicious cycle between obesity and reduced Vitamin D3 levels.

Oxidative stress (OS) plays a key role in the development of various comorbidities among individuals with obesity. Factors contributing to OS in obesity include hyperglycemia, hyperlipidemia, deficiencies in vitamins and minerals, chronic low-grade inflammation, endothelial and mitochondrial dysfunction, among others (Wheatcroft SB et al., 2003; Aeberli I. et al., 2011; Manna P. et al., 2015). OS-induced overproduction of reactive oxygen species (ROS) and reactive aldehyde derivatives leads to a decrease in cellular ATP, NAD^+, and glutathione (GSH) levels, resulting in DNA, lipid, and protein damage, and ultimately triggering cell death (Rolo AP et al., 2012). In vitro, GSH deficiency causes downregulation of VDBP/VD-25-hydroxylase/VDR and PGC-1α/VDR/GLUT-4 in myotubes, and upregulation of CYP24a1 in hepatocytes (Jain SK et al., 2018). Vitamin D binding protein (VDBP) is essential for efficient transport, while VD-25-hydroxylase is required for the hydroxylation of cholecalciferol. Our results demonstrate that SAM administration leads to increased serum levels of Vitamin D3 (Figure 16). The proposed mechanism for this effect is that SAM, as a precursor of the amino acid cysteine, enhances GSH production, which reduces oxidative stress and upregulates VDBP/VD-25-hydroxylase/VDR, thereby increasing Vitamin D3 bioavailability and attenuating the inflammatory process (Jain SK et al., 2018).

In our study, we observed a significant decrease in serum Vitamin D3 (25(OH)D) levels associated with an increase in the TyG index in experimental animals with fructose-induced obesity, as well as a negative correlation between the TyG index and Vitamin D3 levels (Figure 17). The primary physiological effects of Vitamin D include maintaining bone metabolism homeostasis by facilitating calcium and phosphorus absorption and inhibiting parathyroid hormone secretion (Carlberg et al., 2023). With the discovery of vitamin D receptors in multiple tissues and cells, additional biological effects of Vitamin D have been recognized, including stimulation of insulin production, improvement of glucose uptake, and upregulation of UCP3 (Abbas et al., 2017; Fan et al., 2016). However, other studies suggest that Vitamin D supplementation does not influence insulin secretion or the development of type 2 diabetes (Gulseth et al., 2017). Cojic et al. demonstrated that daily oral Vitamin D intake improves HbA1c levels and reduces protein oxidation products at higher doses of Vitamin D (Cojic et al., 2021). They also found that Vitamin D supplementation improves endothelial dysfunction in diabetic patients by reducing ROS production and suppressing inflammation (Cojic et al., 2020).

In our experimental model of fructose-induced obesity, we found a significant negative correlation between Vitamin D3 levels and the TyG index, which reflects the degree of insulin resistance, suggesting that these two parameters are functionally linked (Figure 17).

Although numerous studies have demonstrated the role of Vitamin D in the pathogenesis of insulin resistance (IR), expressed by the TyG index, or type 2 diabetes, few studies focus on the role of insulin resistance in the development of Vitamin D deficiency (Xiang Q et al., 2024). It has been established that adipose tissue, particularly visceral fat, is the main depot for circulating 25(OH)D (Derbel et al., 2025; Alzohily et al., 2024). Individuals with obesity and overweight are known to have lower circulating 25(OH)D levels, likely due to its sequestration in adipose tissue. The mechanisms linking low Vitamin D3 levels with obesity and IR are diverse, including impaired metabolism (Wamberg et al., 2013), reduced storage capacity (Wortsman et al., 2000), and diminished release of Vitamin D (Di Nisio et al., 2017). Several studies have shown that a high TyG index is associated with an increased risk of Vitamin D3 deficiency (Xiang Q et al., 2024; Xiang Q et al., 2023). This finding is corroborated in our experimental model, where obese rats on a high-fructose diet with the highest TyG index values exhibited markedly lower Vitamin D levels. Based on these data, it is suggested that a high TyG index, reflecting insulin resistance, may contribute to the development of Vitamin D deficiency in obese individuals.

In conclusion, in our model of fructose-induced obesity, the TyG index is negatively correlated with serum 25(OH)D levels, with higher index values associated with a greater prevalence of Vitamin D deficiency. These findings suggest that the TyG index, as a marker of insulin resistance, may play a role in the pathogenesis of Vitamin D deficiency, highlighting the need for further studies to elucidate the underlying mechanisms.

2. Inflammation Induced by High-Fructose Diet and Modulation by SAM: Implications for Endothelial, Renal, and Cardiovascular Dysfunction

2.1. Assessment of Serum Tumor Necrosis Factor-α (TNF-α) and C-Reactive Protein (CRP) Levels

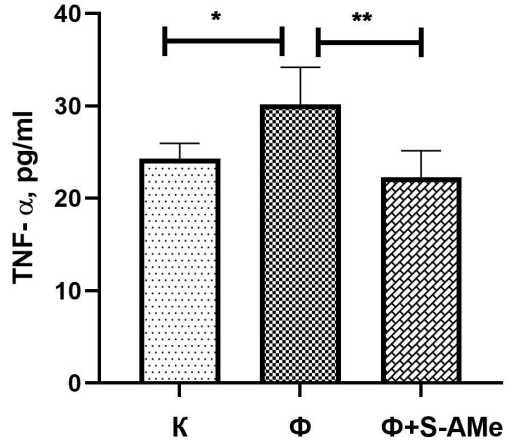

Fig. 18. Changes in Serum TNF-α Levels

*Legend: Data are presented as mean ± standard error of the mean (SEM), (n=6). K – control group; Ф – high-fructose diet (HFD) group; Ф+S-AMe – HFD group supplemented with S-adenosylmethionine; *p<0.05; **p<0.01, t-test.*

Serum TNF-α levels were significantly elevated in the high-fructose diet (HFD) group compared to the control group (*p<0.05). Additionally, a significant reduction in TNF-α levels was observed in the HFD group supplemented with S-adenosylmethionine (S-AMe) compared to the HFD group alone (**p<0.01) (Fig. 18).

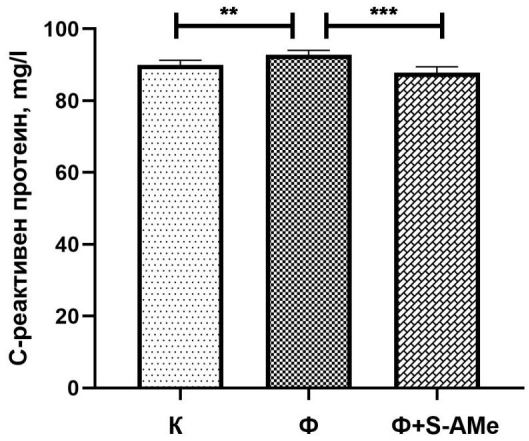

*Fig. 19. Changes in serum C-reactive protein (CRP) levels. Legend: Data are presented as mean ± standard error of the mean (SEM), (n=6). K – control group; Ф – high-fructose diet (HFD) group; Ф+S-AMe – HFD group supplemented with S-adenosylmethionine; **p<0.01; ***p<0.001, t-test.*

Our results demonstrate a significant increase in serum C-reactive protein (CRP) levels in the high-fructose diet (HFD) group compared to the control group (**p<0.01). Supplementation with exogenous S-adenosylmethionine (S-AMe) significantly reduced CRP levels relative to the HFD group (***p<0.001) (Fig. 19).

2.2 Discussion

Inflammation is recognized as a key driver in the development of insulin resistance (IR) and metabolic syndrome. In our study, serum levels of TNF-α and CRP were significantly elevated in the high-fructose diet (HFD) group compared to controls, reaching statistical significance. Conversely, exogenous S-adenosylmethionine (SAM) administration led to a statistically significant reduction in TNF-α and CRP levels relative to the HFD group (Figs. 18 and 19).The fructose-induced elevation of these pro-inflammatory markers observed in our study is likely mediated by specific fructose metabolism, oxidative stress, and visceral adipose tissue hypertrophy. Elevated TNF-α levels contribute to the progression of low-grade hepatic inflammation and apoptosis, while directly impairing insulin signaling through dysregulation of

serine and tyrosine phosphorylation of IRS-1, thereby inducing insulin resistance in both hepatic and peripheral tissues (Ibrahim SM et al., 2015).

TNF-α is a principal pro-inflammatory cytokine that plays a central role in modulating the inflammatory response by stimulating NF-κB expression. This activation not only enhances the secretion of pro-inflammatory cytokines (TNF-α, IL-1, IL-6) and CRP but also promotes the generation of reactive oxygen species (ROS) (Tilg et al., 2000). CRP serves as another key inflammatory biomarker, primarily synthesized in response to IL-6 and, to a lesser extent, IL-1 and TNF-α. Its main function is the activation of C1q in the complement system, facilitating opsonization of pathogens and cell-mediated immunity. Additionally, CRP activates Fc-γ receptors, stimulating the production of pro-apoptotic cytokines and inflammatory mediators (IL-1β, TNF-α, ROS), thereby creating a feedback loop that amplifies the inflammatory response (Devaraj et al., 2005).

Due to its specific glycolytic metabolism, fructose promotes increased formation of trisaccharides, which indirectly enhance the generation of advanced glycation end-products (AGEs) via the Maillard reaction (Gaens et al., 2013). Binding of AGEs to their receptor (RAGE) activates multiple signaling pathways, including MAPKs, STAT3, and Akt (Hudson et al., 2018). These signaling cascades further induce downstream effectors such as NF-κB and EGR-1 (Xie et al., 2013). The AGE-RAGE interaction results in intracellular oxidative stress and an amplified inflammatory response, with elevated levels of TNF-α, CRP, MCP-1, and IL-6, thereby perpetuating the cycle of AGE formation and pro-inflammatory signaling (Rai et al., 2019). Dietary fructose intake is closely associated with the development of visceral obesity, adipose tissue dysfunction, and dysregulation of adipokine secretion. According to Taylor et al. (2021), adipose tissue hypertrophy following fructose overload exhibits pro-inflammatory characteristics, including increased secretion of leptin, TNF-α, IL-6, and MCP-1, alongside reduced secretion of adiponectin, IL-10, and IL-4. Fructose-induced hyperuricemia further suppresses adiponectin levels, limiting its capacity to inhibit hepatic gluconeogenesis and adipose tissue inflammation, or to enhance β-oxidation in the liver and skeletal muscle, thereby sustaining the obesogenic phenotype (Chait et al., 2020).

High fructose consumption also triggers oxidative stress (OS) through multiple pathways, such as reduced catalase mRNA expression (Cavarape et al., 2001) and decreased Cu/Zn SOD levels (Poznyak et al., 2020), increased activity of NADPH oxidase and xanthine oxidase (Berry et al., 2004), and elevated production of TNF-α and CRP, which collectively promote ROS generation and cellular damage (Tilg et al., 2000). Additionally, Liao et al. (2020) demonstrated that OS can modulate TNF-α levels via advanced oxidation protein products (AOPPs), a family of oxidized tyrosine-containing protein derivatives similar to AGEs, which serve as biomarkers of oxidative stress (Witko-Sarsat et al., 1996). AOPPs were shown to enhance TNF-α and IL-1β production in chondrocytes via a NADPH oxidase 4-dependent, p38-MAPK-mediated pathway. Furthermore, treatment with the NADPH oxidase inhibitor apocynin reduced ROS production in the adipose tissue of KKAy mice, leading to increased adiponectin expression and decreased TNF-α levels (Furukawa et al., 2004). These findings indicate that mitigating oxidative stress in adipose tissue can restore adipokine balance in vivo..

In line with these observations, our study demonstrated that SAM supplementation significantly reduced TNF-α and CRP levels, indicating that this exogenous antioxidant protects peripheral tissues and the liver by suppressing pro-inflammatory signaling pathways and cytokine synthesis, thereby mitigating insulin resistance, chronic low-grade inflammation, oxidative stress, and excessive release of free fatty acids.

3. Interplay Between OS, Inflammation, and ED in a HFD Model and the Effects of SAM Supplementation

3.1. Variations in morphometric parameters of the left ventricle and interlobar arteries in a HFD model and changes following SAM supplementation

3.1.1 Results from the macroscopic examination of the heart and renal interlobar arteries

Upon autopsy of the experimental animals, visible macroscopic changes in adipose tissue distribution were observed. In the high-fructose diet (HFD) group, a greater amount of visceral adipose tissue was noted compared to the control group. Rats subjected to HFD with SAM supplementation exhibited a noticeable reduction in visceral fat accumulation compared to the HFD-only group (Fig. 20). Careful examination of the hearts revealed pronounced hypertrophy in the HFD group relative to controls. In contrast, HFD rats receiving SAM supplementation showed less pronounced cardiac hypertrophy (Fig. 20).

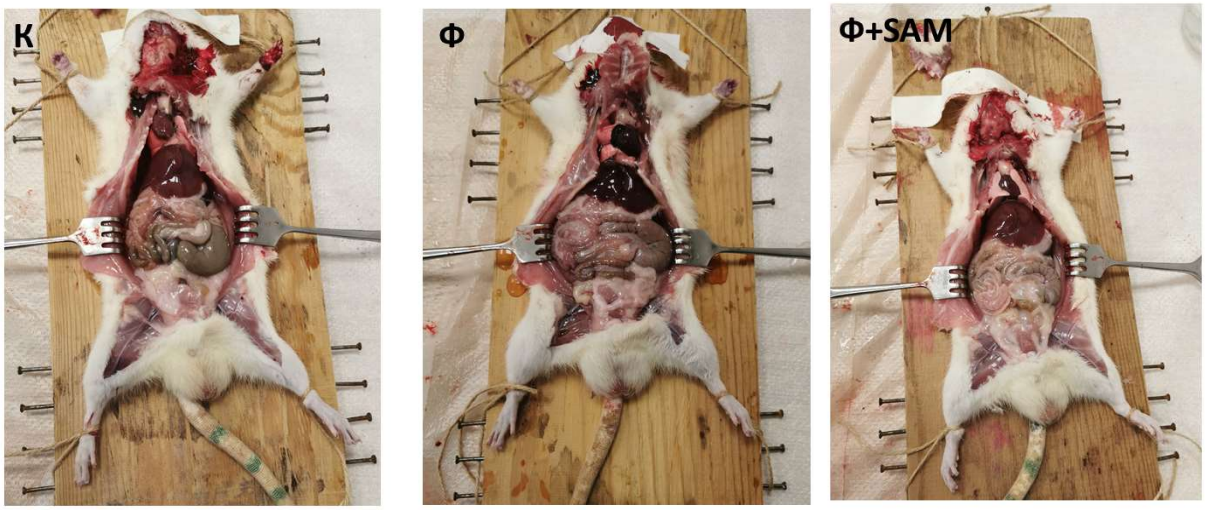

Fig. 20. Macroscopic changes in visceral adipose tissue (VAT) distribution among the experimental groups. Legend: K – control group; Ф – HFD group; Ф+S-AMe – HFD group supplemented with S-adenosylmethionine

3.1.2 Results from the histological and morphometric analysis of the left ventricle

The results from routine histological analysis of cardiomyocytes in control group rats demonstrated preserved cellular architecture and normal nuclear morphology (Fig. 21).

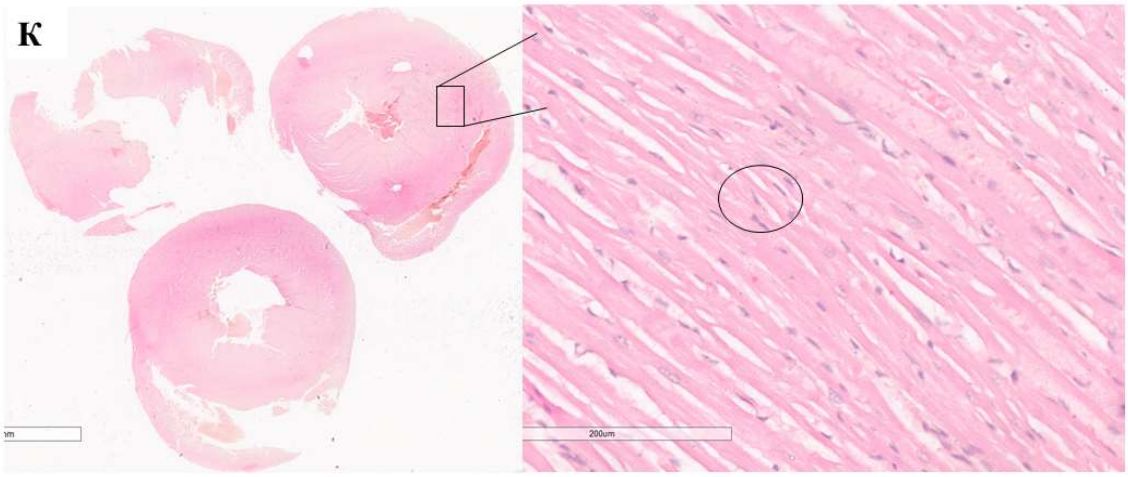

Fig. 21. Histological analysis of the left ventricular myocardium in a control group rat. Hematoxylin-eosin staining. Magnification ×20 (Aperio ImageScope – v12.3.3.5048). Legend: K – control group

In contrast to the control group, the high-fructose diet (HFD) group exhibited alterations in cardiomyocyte architecture. Features of hypertrophy were observed, including cytoplasmic enlargement, marked nucleomegaly with unevenly dispersed chromatin, nuclear atypia (boxcar nuclei), and expansion of connective tissue (Fig. 22).

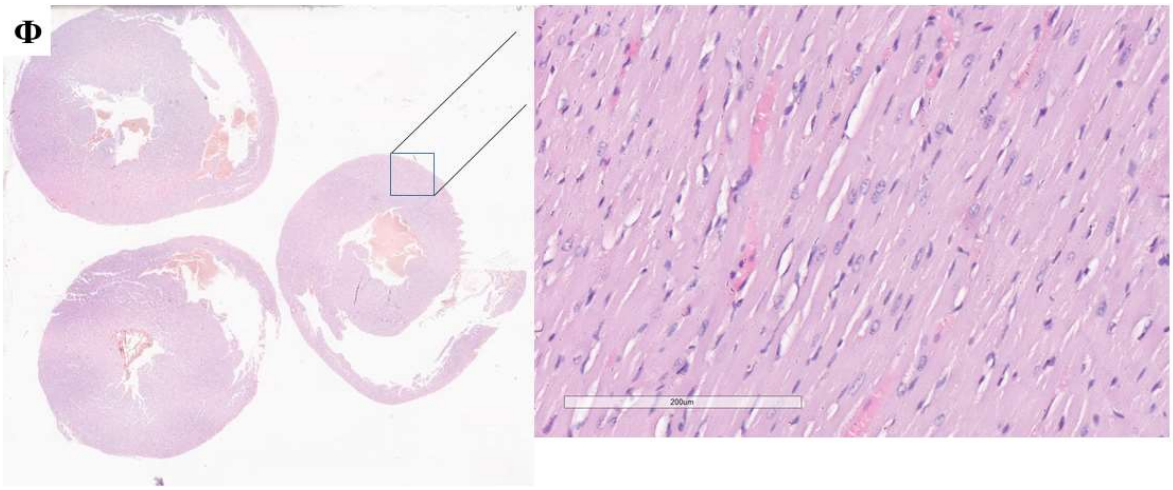

Figure 22. Histological analysis of left ventricular myocardium in a rat from the high-fructose diet (HFD)

group. Hematoxylin-eosin staining. Magnification ×20 (Aperio ImageScope – v12.3.3.5048) Legend: F – fructose group

The histological analysis of cardiomyocytes from rats subjected to a high-fructose diet with SAM supplementation revealed milder pathomorphological changes in the left ventricular myocardium compared to the fructose-only group. Occasional nuclear atypia and nucleomegaly were still observed, but these features were significantly less frequent than in the fructose group (Fig. 23).

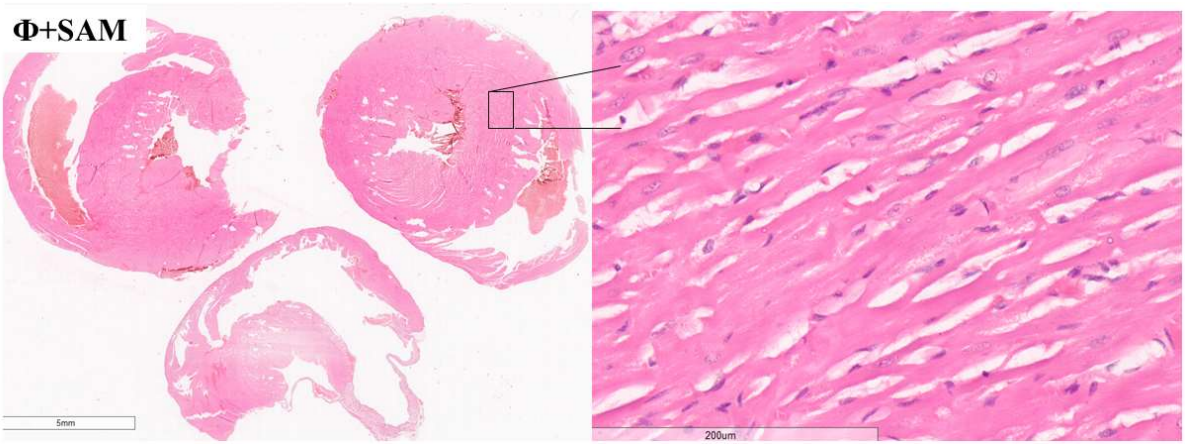

Fig. 23. Histological analysis of the left ventricular myocardium from a rat in the high-fructose diet group with SAM supplementation. Hematoxylin-eosin staining. Magnification ×20 (Aperio ImageScope – v12.3.3.5048). Legend: Ф+SAM – high-fructose diet group with SAM supplementation.

Morphometric analysis of hematoxylin-eosin–stained cardiac sections revealed a statistically significant increase in left ventricular wall thickness in the high-fructose diet (HFD) group compared to controls (**p<0.01). SAM supplementation in HFD animals led to a statistically significant reduction in left ventricular thickness compared to the HFD group (*p<0.05), with values approaching those of the control group (Fig. 24).

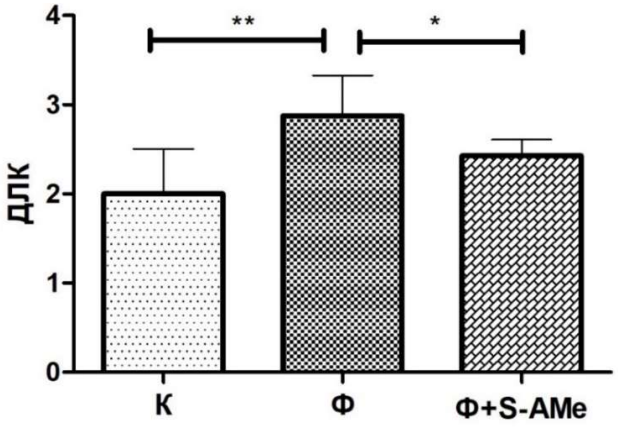

Fig. 24. Morphometric analysis of the left ventricle. Legend: Data are presented as mean ± standard error

*of the mean (SEM), n=6. LVWT – left ventricular wall thickness; K – control group; F – high-fructose diet group; F+SAM – HFD group supplemented with S-adenosylmethionine; *p<0.05; **p<0.01, t-test.*

3.1.3 Results from the histological and morphometric analysis of the interlobar branches of the renal artery

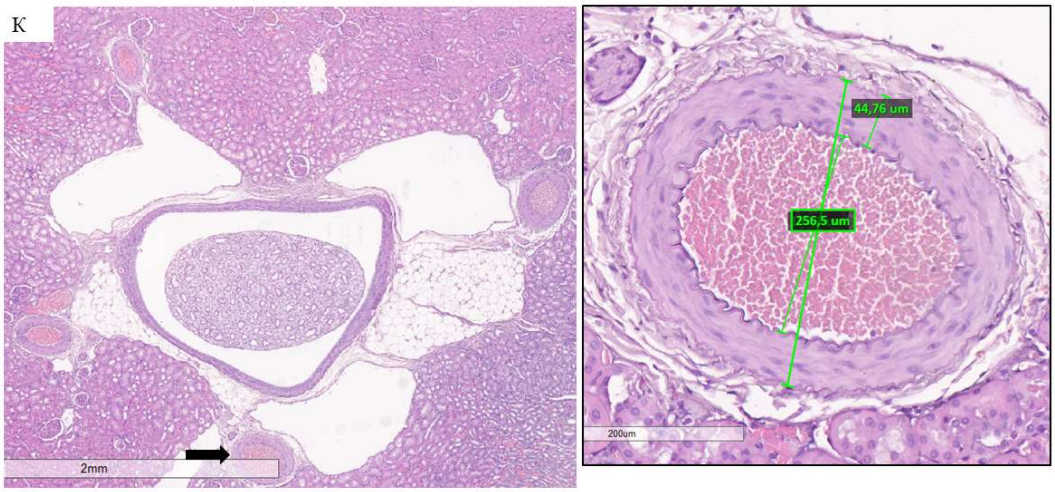

Fig. 25. Histological analysis of an interlobar branch of the renal artery. Hematoxylin-eosin staining. Magnifications ×2 and ×20 (Aperio ImageScope – v12.3.3.5048) Legend: K – control group

The results from the routine histological analysis of the interlobar artery in rats from the control group demonstrate preserved architecture of the endothelial cells and the vascular wall (Fig. 25).

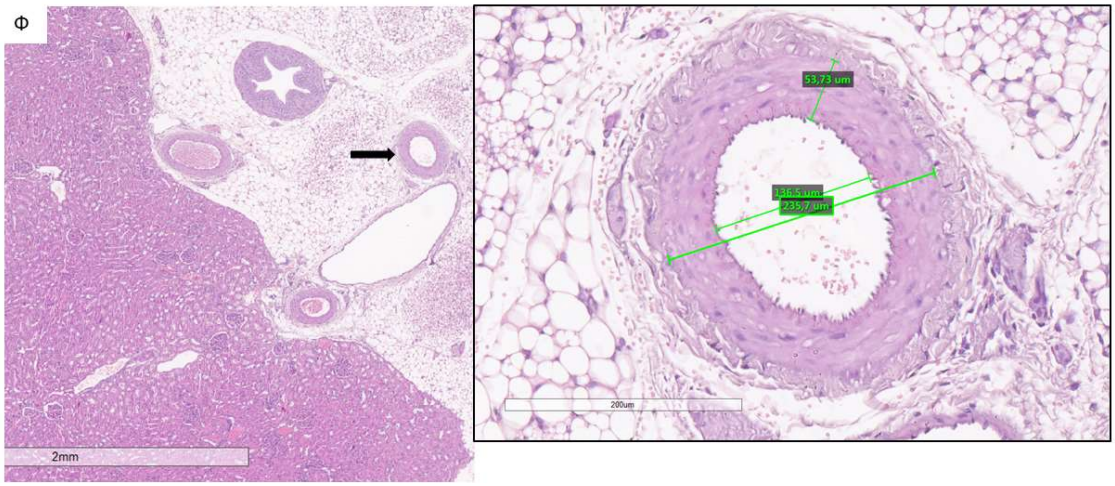

Fig. 26. Histological analysis of an interlobar branch of the renal artery. Hematoxylin-eosin staining. Magnification ×2 and ×20 (Aperio ImageScope – v12.3.3.5048) Legend: Ф – fructose group

In the fructose-fed (FFD) group, alterations in the tunica intima were observed, characterized by swelling of the subendothelial space and vacuolization of endothelial cells. Compared to the control group, FFD rats exhibited hypertrophy of vascular smooth muscle cells (VSMCs) with areas of elastic fiber fragmentation and smoothing, accompanied by connective tissue proliferation and remodeling of the vascular wall (Fig. 26). Our histological findings correspond to the morphometric changes presented in Table 3, including thickening of the vascular wall and changes in the internal diameter. Additionally, the fructose group displayed glomerular hypertrophy, glomerulosclerosis, signs of interstitial fibrosis, and focal interstitial infiltration by mononuclear cells (Fig. 26).

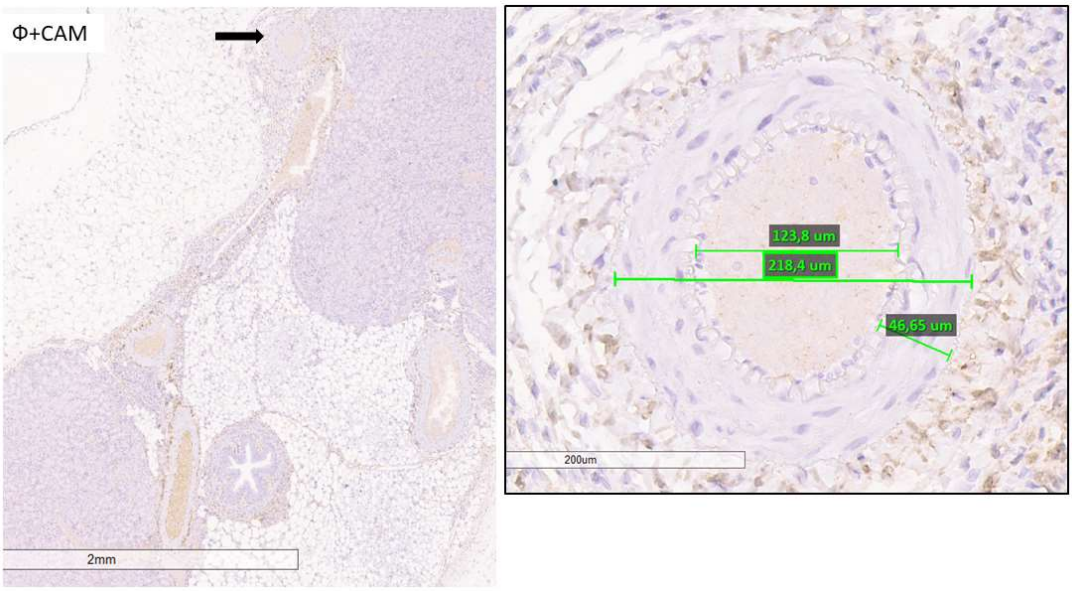

Fig. 27. Histological analysis of an interlobar branch of the renal artery. Hematoxylin-eosin staining. Magnification ×2 and ×20 (Aperio ImageScope – v12.3.3.5048) Legend: Φ+SAM – fructose-fed group with SAM supplementation

The histological analysis of the interlobar artery in fructose-fed rats supplemented with SAM revealed milder pathological changes compared to the fructose-only group. In the tunica intima, swelling of the subendothelial space and vacuolization of endothelial cells were still present, but markedly less pronounced than in the fructose group. Signs of vascular wall thickening, interstitial fibrosis, and mononuclear cell infiltration were occasionally observed, yet to a significantly lesser extent than in the fructose-fed group (Fig. 27).

Morphometric parameters of interlobar arteries (kidney)	C	F	F+S-AMe
Extrinsic diameter (μm)	201,8 ± 11.42	245.8± 13.58*	224.5± 12,64
Intrinsic diameter (μm)	104.1± 13.86	150.1± 10,69 *	128.0± 16.62
Ratio of tunica media thickness to internal diameter (μm)	0.74± 0.05	0.75± 0.05	0.54± 0.05 #

Table 3. Morphometric parameters measured in the interlobar arteries of the kidney.
Legend: Data are presented as mean ± standard error of the mean (SEM), (N=6). K – control group; F – high-fructose diet (HFD) group; F+S-AMe – HFD group supplemented with S-adenosylmethionine. . p<0.05 – statistically significant difference between K and F groups; # p<0.05 – statistically significant difference between F and F+S-AMe groups. Aperio Image Scope (v12.3.3.5048).*

The results of the morphometric analysis of the interlobar branches of the renal artery revealed statistically significant differences between the experimental groups. The internal and external diameters in the HFD group were significantly increased compared to the control group (*p<0.05). In the HFD + SAM group, the diameters were narrower than in the HFD group, although the differences were not statistically significant. The ratio of tunica media thickness to internal diameter in the HFD group showed no significant change compared to controls, whereas in the SAM-supplemented group, this ratio was significantly reduced compared to the HFD group (#p<0.05) (Table 3).

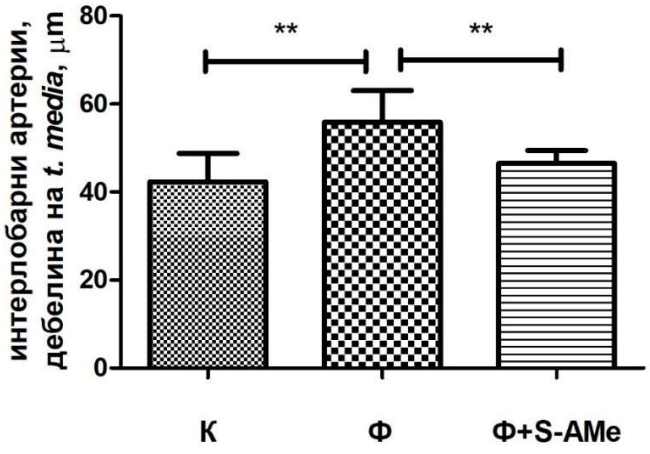

Fig. 28. Changes in tunica media thickness of the interlobar arteries. Legend: Data are presented as mean ± standard error of the mean (SEM), (N=6). K – control group; Ф – HFD group; Ф+S-AMe – HFD group

*supplemented with S-adenosylmethionine; **p<0.01 – statistical significance between the control and HFD groups, and between the HFD and HFD+SAM groups.*

The analysis of tunica media thickness in the interlobar arteries revealed statistically significant differences between the experimental groups. Rats in the HFD group exhibited increased wall thickness compared to the control animals (**p<0.01). In contrast, HFD rats supplemented with SAM showed significantly reduced wall thickness compared to the HFD group (Fig. 28).

3.1.4 Discussion

We hypothesize that fructose-induced left ventricular hypertrophy results from several potential mechanisms: (1) impaired β-oxidation, (2) hepatic de novo lipogenesis with increased flux of fatty acids to the heart, and/or (3) enhanced lipid synthesis within the myocardium. In a study by Zhang et al. (2024) on HFD-fed mice, an increase in malonyl-CoA, a carnitine-palmitoyltransferase 1 (CPT1) inhibitor, was observed, directly suppressing CPT1-mediated fatty acid oxidation in the heart. The same study also reported upregulation of 3-hydroxy-3-methylglutaryl-CoA reductase (HMGCR) phosphorylation and increased levels of the endogenous AMPK activator, 5-aminoimidazole-4-carboxamide ribonucleotide (AICAR). These findings suggest that excessive fructose intake suppresses cardiac fatty acid oxidation through alterations in the AMPK–ACC axis, leading to myocardial lipid accumulation, systolic dysfunction, and left ventricular hypertrophy.

Despite the isomeric similarities between fructose and glucose, fructose absorption and metabolism proceed much more rapidly and in an uncontrolled manner due to the lack of inhibition by phosphofructokinase, which may be a key factor underlying metabolic dysregulation in the heart. A dual in vivo isotope experiment by Zhang et al. demonstrated that β-oxidation is suppressed due to rapid competition for oxygen during fructose catabolism. Moreover, fructolysis generates less ATP compared to β-oxidation, suggesting that this energy deficit may be a primary driver of left ventricular hypertrophy and, subsequently, heart failure.

Another potential contributor to the development of hypertrophy in our experimental animals is fructose-induced obesity. Numerous studies have established a link between increased body weight and chronic elevation of blood pressure. A meta-analysis by Friedemann et al. (2012) reported that children with obesity exhibit higher levels of serum lipids, glucose, and insulin compared to age-matched children with normal weight. These metabolic risk factors contribute to the development of cardiovascular diseases, including atherosclerosis, left ventricular hypertrophy (LVH), and renal vascular damage. Left ventricular hypertrophy represents an advanced form of cardiac remodeling, characterized by an increase in left ventricular mass due to wall thickening or abnormal chamber dilation. This altered cardiac geometry is associated with ventricular arrhythmias, heart failure, and a fourfold increase in cardiovascular morbidity and mortality (de Simone et al., 1995). Multiple mechanisms underlie the development of LVH in obesity (Fig. 29). Metabolic dysfunction plays a central role in obesity-associated left ventricular

remodeling (Brady et al., 2016). As body weight increases, energy storage demands rise, leading to adipocyte hypertrophy. Over time, classically activated macrophages and T lymphocytes infiltrate the expanding adipose tissue, triggering a robust inflammatory response with cytokine release, oxidative stress, adipocyte necrosis, and endothelial dysfunction, ultimately contributing to organ damage (Brady et al., 2016).

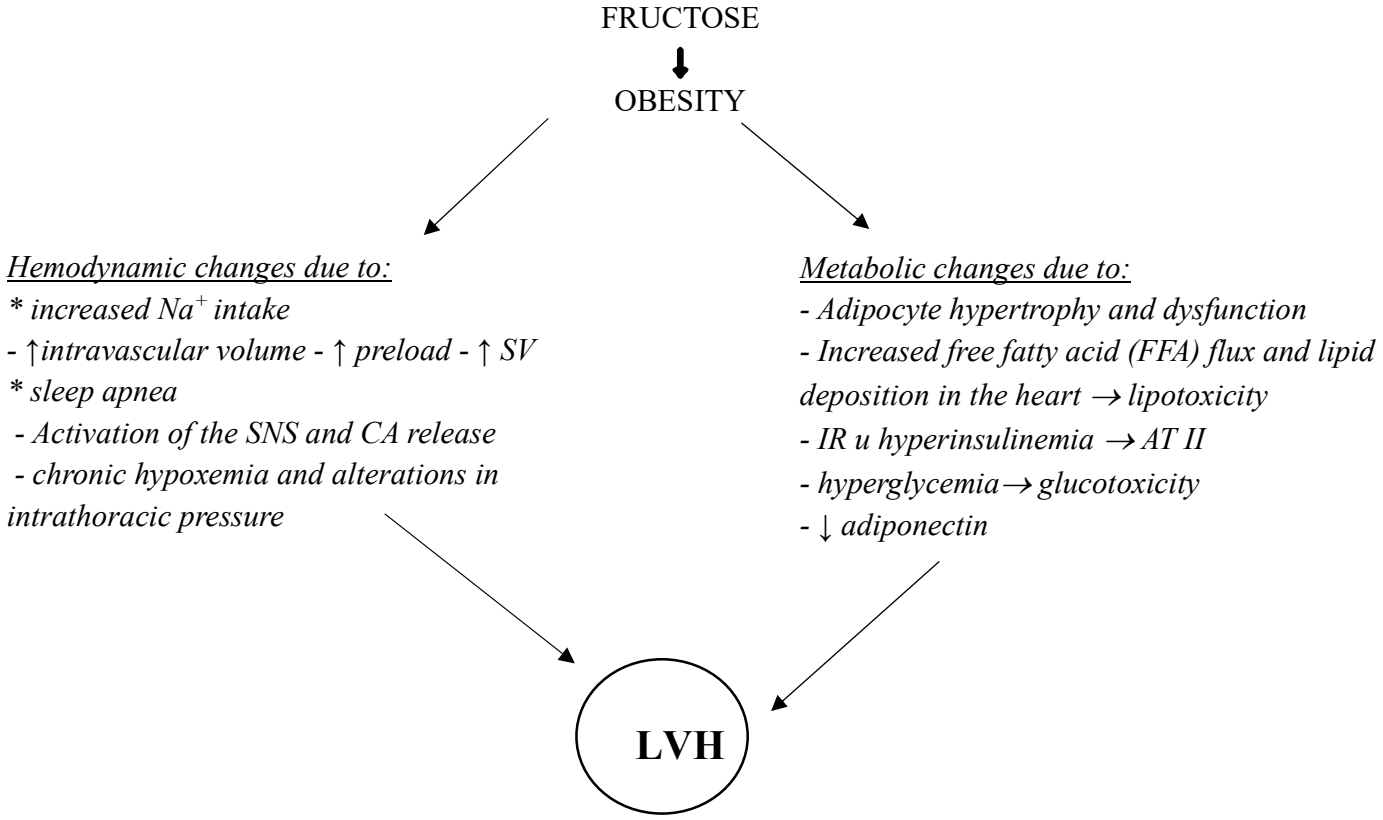

Figure 29. Mechanisms involved in the development of left ventricular hypertrophy in fructose-induced obesity Legend: LVH – left ventricular hypertrophy; SV – stroke volume; SNS – sympathetic nervous system; CA – catecholamines; IR – insulin resistance; Ang II – angiotensin II

Increased hepatic de novo lipogenesis and enhanced influx of free fatty acids exert a lipotoxic effect on pancreatic β-cells, leading to insulin resistance and hyperinsulinemia (Fig. 29). Abnormal insulin regulation activates the sympathetic nervous system and increases the synthesis of angiotensin II, a cardiomyocyte growth factor (Zamolodchikova et al., 2024), which results in myocardial hypertrophy, fibrosis, and apoptosis.

Adipokines are cytokines, hormones, and pro-inflammatory mediators produced by adipose tissue. Their expression is upregulated in obesity, and they contribute to the regulation of the cardiomyocyte extracellular matrix and apoptosis—two key aspects of cardiac remodeling (Brady et al., 2016). It has been established that in obesity, adipose tissue undergoes accelerated cellular and structural remodeling to compensate for excessive energy intake (Senkus et al., 2022). These

adaptations adversely affect adiponectin activity, which plays a crucial role in the pathogenesis of metabolic alterations associated with obesity. Reduced secretion of this adipokine or decreased receptor expression leads to insulin resistance and contributes to the development of left ventricular hypertrophy due to the loss of its protective effects against inflammation, endothelial dysfunction, and oxidative stress. Another possible mechanism contributing to left ventricular hypertrophy is elevated blood pressure. Insulin resistance and chronic systemic inflammation in obesity are associated with endothelial dysfunction and vasoconstriction, resulting in increased blood pressure, elevated afterload, and the development of LVH (Hall et al., 2015). Another adipokine with a significant role in obesity is leptin. Notably, individuals with obesity exhibit elevated leptin levels but remain resistant to its protective effects. Hyperleptinemia and leptin resistance have been shown to lead to adverse cardiac outcomes, including increased levels of reactive oxygen species in the heart, cardiomyocyte apoptosis, and cardiac hypertrophy (Ouchi et al., 2011).

Oxidative stress and chronic inflammation (elevated TNF-α levels) play a pivotal role in the pathogenesis of myocardial remodeling, including hypertrophy, fibrosis, apoptosis, and contractile dysfunction. Supporting this notion are the results of our study, in which SAM administration was associated with a reduction in the degree of left ventricular hypertrophy through suppression of oxidative stress (Fig. 24). This finding is further corroborated by Jalgaonkar SV et al., who demonstrated that SAMe intake reduces TNF-α levels and increases glutathione (GSH) levels, thereby preventing cardiomyocyte damage and inflammatory infiltration of the myocardium (Jalgaonkar SV et al., 2024). A study by Yuanchen et al. (2022), aimed at evaluating the cardioprotective effect of SAMe in a myocardial infarction model, showed a reduction in cardiac fibrosis and an increase in angiogenesis. According to the authors, suppression of myocardial fibrosis by SAMe treatment may be attributed to the expression of Jagged1 and Notch1 in the rat myocardium, which promotes angiogenesis (Yuanchen et al., 2022).

In the present study, we also investigated the effect of fructose loading on the morphology of the interlobar branches of the renal artery. Morphometric analysis revealed a statistically significant increase in tunica media thickness in the FRU group compared with the control group. In contrast, SAM supplementation resulted in a statistically significant reduction in tunica media thickness compared with the FRU group (Fig. 28). A potential cause of interlobar artery (preglomerular artery) thickening in our experimental animals is the development of fructose-induced metabolic syndrome. Epidemiological data indicate that metabolic syndrome may serve both as a risk factor for renal injury and as a predictor of adverse outcomes in patients with chronic kidney disease (Kambham N et al., 2001). In this context, we found that increased fructose intake led to hypertrophic changes in the kidney and interlobar arteriopathy, manifested by thickening of the tunica media and enlargement of both the internal and external arterial diameters (Table 3, Fig. 28). Hyperuricemia is considered one of the components of metabolic syndrome that induces vascular injury, characterized by thickening of the interlobar arteries and proliferation of vascular smooth muscle cells (VSMCs). Rao et al. demonstrated that uric acid stimulates the expression of the PDGF-A chain and mediates cellular proliferation in cultured vascular smooth muscle cells (Rao GN et al., 1991). This finding was further confirmed by Kang et al. (2002), who reported increased de novo expression of COX-2 mRNA, thromboxane A2

(TXA2), and enhanced proliferation of vascular smooth muscle cells following incubation with uric acid. Upon entering vascular smooth muscle cells, uric acid activates nuclear transcription factors (NF-κB and AP-1), thereby shifting the cellular phenotype toward a pro-inflammatory and proliferative state (Fig. 30). Administration of a COX-2 inhibitor or a TXA2 receptor antagonist prevents vascular smooth muscle cell proliferation, providing evidence for the role of uric acid as a mitogenic factor.

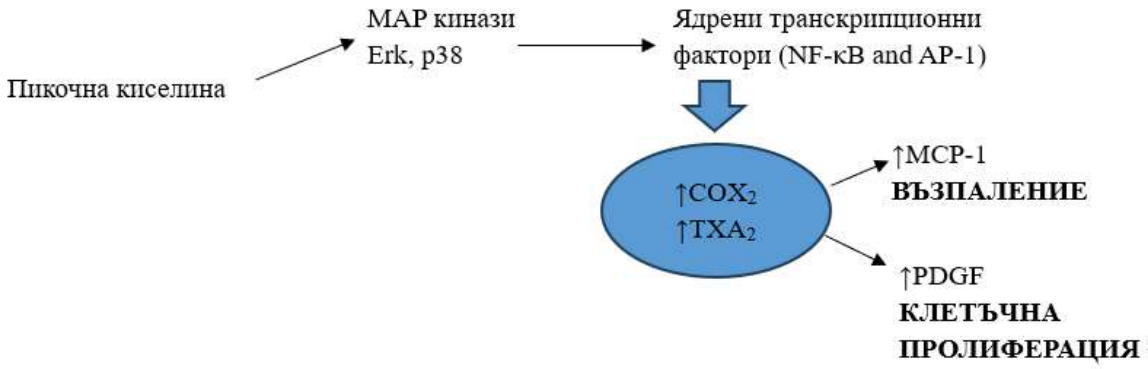

Fig. 30. Molecular pathways through which uric acid induces inflammation and cellular proliferation. Legend: MAP – mitogen-activated protein; NF-κB – nuclear factor kappa B; AP-1 – activator protein-1; COX-2 – cyclooxygenase-2; TXA_2 – thromboxane A_2; MCP-1 – monocyte chemoattractant protein-1; PDGF – platelet-derived growth factor.

Another possible mechanism underlying interlobar arterial arteriopathy is the elevated levels of angiotensin II (Ang II), which plays a key role in vascular alterations induced by a high-fructose diet in rats. According to Sánchez-Lozada LG et al. (2005; 2007), Ang II contributes to the development of hypertension, suppression of adiponectin secretion (Ran J et al., 2006), adipocyte hypertrophy (Furuhashi M et al., 2004), and induction of oxidative stress (Shinozaki K et al., 2004). These findings are further supported by Hsieh PS (2005), who demonstrated that inhibition of Ang II suppresses vascular smooth muscle cell proliferation, restores endothelial nitric oxide synthase (eNOS) activity, and improves insulin sensitivity.

The intake of a high-fructose diet increases uric acid levels, which has been shown to inhibit nitric oxide synthase and reduce endothelial nitric oxide (NO) bioavailability (Gersch et al., 2008). This adversely affects vascular regulation and leads to vascular inflammation, endothelial dysfunction, oxidative stress, and arterial hypertension (Russo et al., 2020; Nakagawa et al., 2005).

Thickening of the preglomerular arterial wall results in increased afferent vascular resistance, which in turn reduces glomerular plasma flow and triggers activation of the renin–angiotensin–aldosterone system (RAAS), ultimately leading to the development of systemic arterial hypertension. Systemic hypertension itself is a well-established pathogenetic factor for damage to renal vessels and the interstitium. This process is mediated through multiple mechanisms, including further activation of the RAAS, endothelial dysfunction, podocyte injury, increased calcium channel activity, enhanced oxidative stress, overexpression of hypoxia-inducible factor (HIF), and others. These interconnected processes highlight the existence of a vicious pathophysiological cycle between elevated uric acid levels and chronic renal arteriopathy.

3.2. Variations in SOD-1 expression in a HFD and changes following SAM administration

3.2.1 Results from the immunohistochemical analysis of SOD-1 expression in cardiomyocytes

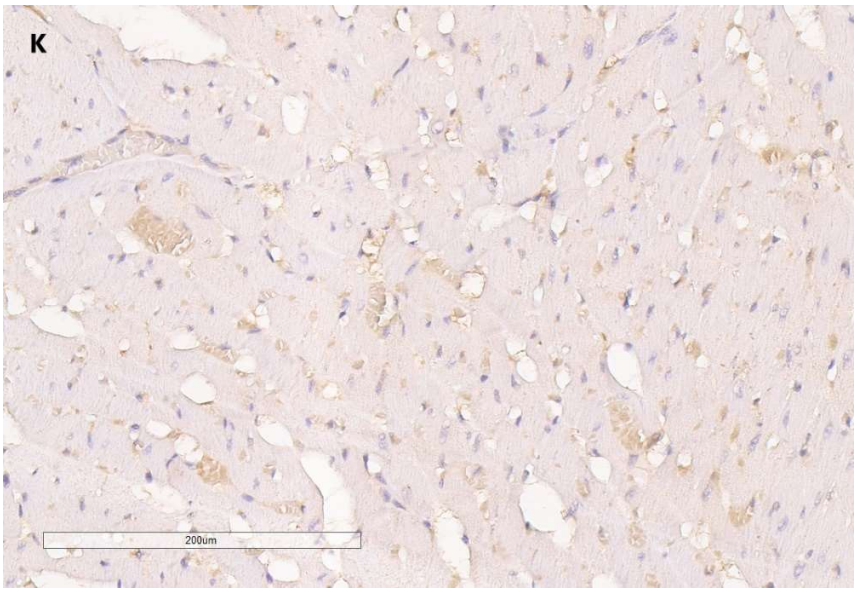

Fig. 31. Immunohistochemical staining for SOD-1 in cardiomyocytes (perinuclear and cytosolic) of control group rats. Magnification: ×20 (Aperio Image Scope – v12.3.3.5048). Legend: K – control group

The immunohistochemical analysis of SOD-1 revealed predominantly moderate expression intensity in the cardiomyocytes of control group rats. Some cells with lower expression levels were also observed among the control animals (Fig. 31).

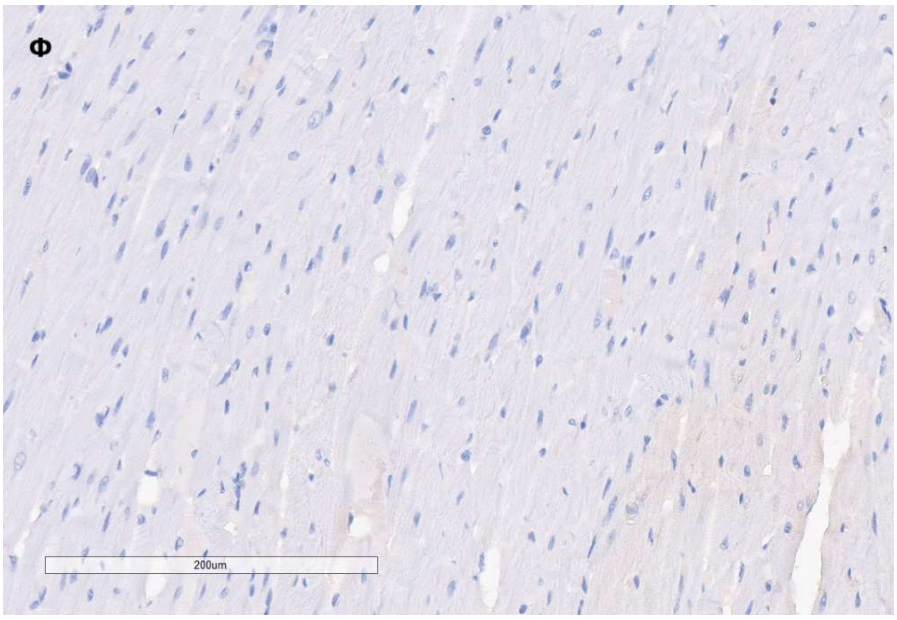

Fig. 32. Immunohistochemical staining for SOD-1 in cardiomyocytes (perinuclear and cytosolic) of rats from the high-fructose diet (HFD) group. Magnification: ×20 (Aperio Image Scope – v12.3.3.5048) Legend: Φ – high-fructose diet rats

Our results show that, compared to the control group, SOD-1 expression in the cardiomyocytes of the high-fructose diet (HFD) group is predominantly absent (Fig. 32).

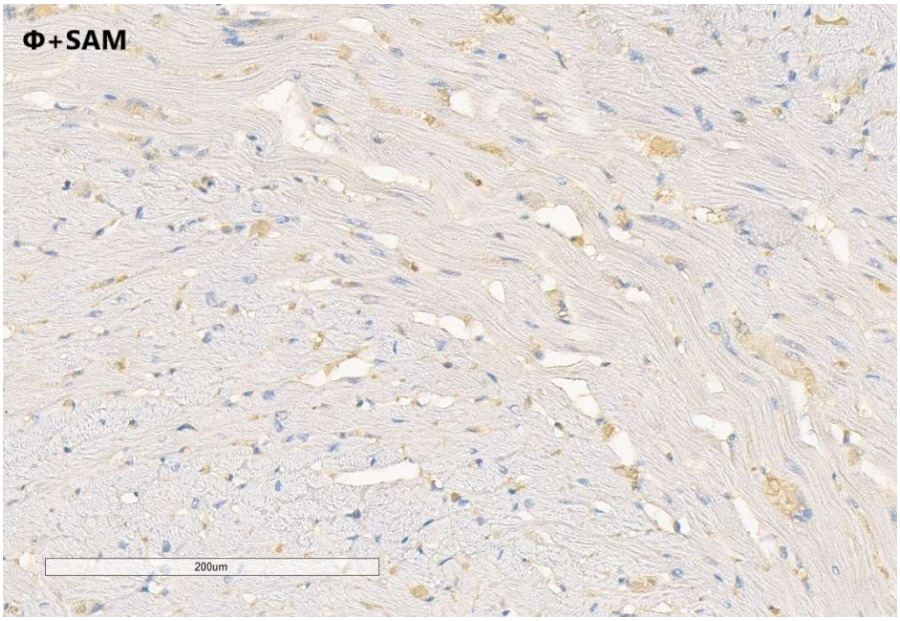

Fig. 33. Immunohistochemical analysis using anti–SOD-1 in cardiomyocytes (perinuclear and cytosolic) of rats from the high-fructose diet (HFD) group treated with SAM. Magnification: ×20 (Aperio Image Scope – v12.3.3.5048) Legend: Φ+SAM – rats on HFD receiving SAM

In contrast to the fructose-only group, the HFD+SAM group shows an increased expression of SOD-1 in cardiomyocytes. Some cells still exhibit weak to absent expression, but cells with moderate and strong expression are more diffusely distributed. The intensity of SOD-1 expression in this group approaches the levels observed in control animals (Fig. 33). Statistical analysis revealed significant differences in SOD-1 expression among the experimental groups (Fig. 34).

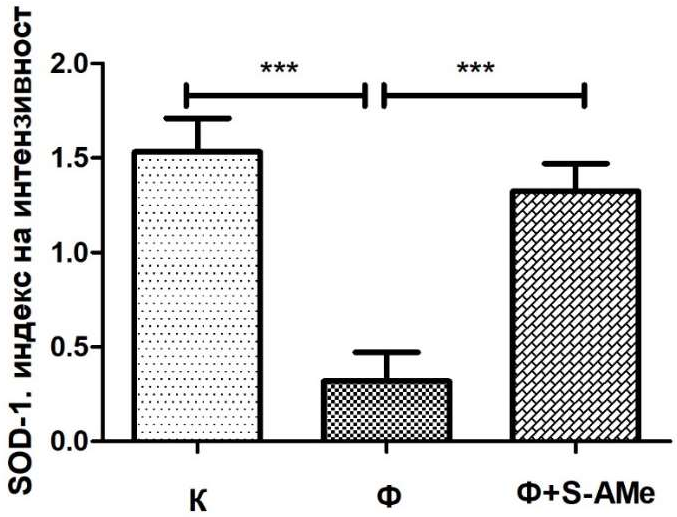

*Fig. 34. Reaction intensity index (RII) of SOD-1 protein in cardiomyocytes of rats from the three experimental groups. Legend: Data are presented as mean ± standard error of the mean (SEM), (n=8); K – control group; F – fructose diet group; F+S-AMe – HFD with S-AMe supplementation; *** – p<0.0001, t-test.*

The results of our study demonstrate a statistically significant lower expression intensity of SOD-1 in rats subjected to a high-fructose diet (HFD) compared to the control group ($p < 0.0001$). In rats receiving HFD combined with S-AMe supplementation, SOD-1 expression was significantly higher, also reaching statistical significance ($p < 0.0001$) (Fig. 34).

3.2.2 Results obtained from the immunohistochemical analysis of SOD-1 expression in the endothelial cells of the interlobar arteries

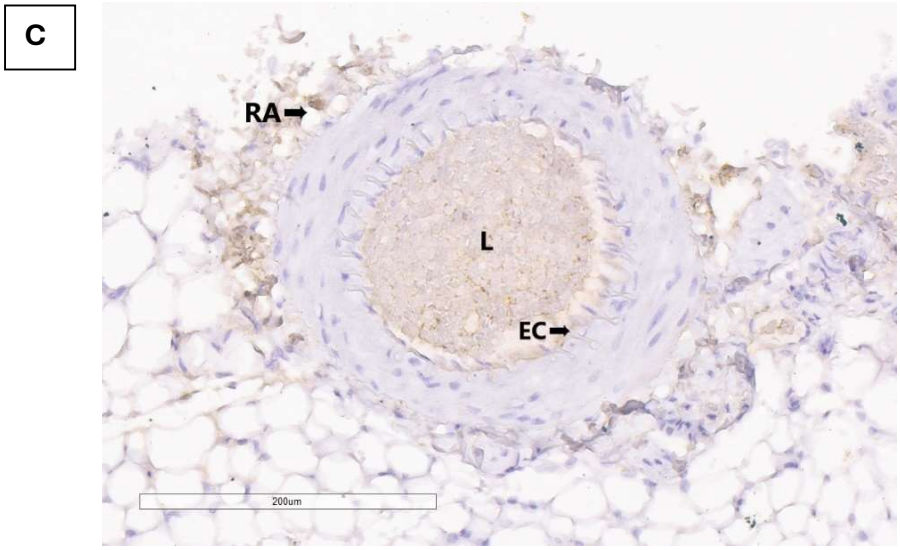

Fig. 35. Immunohistochemical analysis with anti-SOD-1 in endothelial cells of the interlobar branches of the renal artery in rats from the control group. Magnification ×20 (Aperio Image Scope – v12.3.3.5048)
Legend: C – control group; RA – interlobar branch of the renal artery; L – lumen; EC – endothelial cells

Our results show predominantly weak to absent SOD-1 expression intensity in the endothelial cells of the interlobar branches of the renal artery in the control group of experimental animals (Fig. 35).

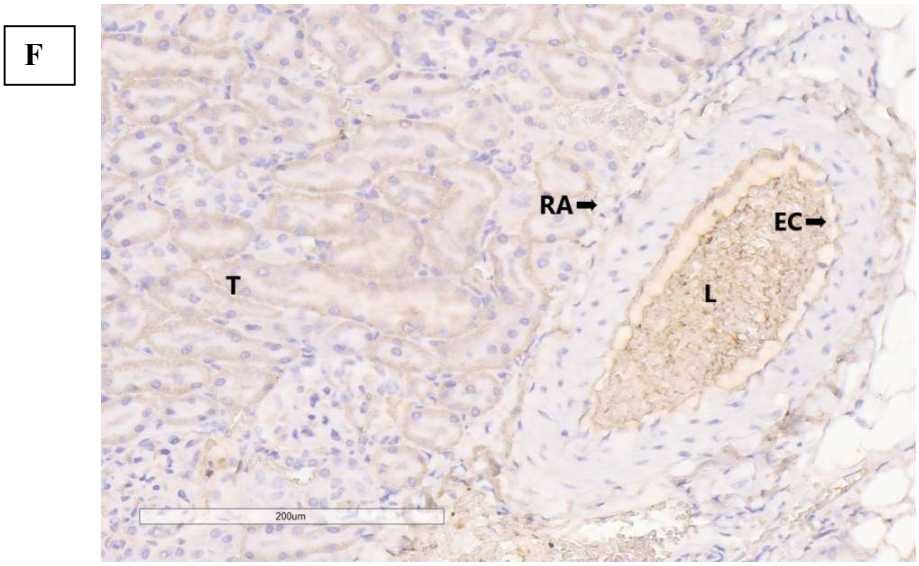

Fig. 36. Immunohistochemical analysis using anti-SOD-1 in the endothelial cells of the interlobar

branches of the renal artery in rats from the fructose diet group. Magnification ×20 (Aperio Image Scope – v12.3.3.5048). Legend: F – fructose diet group; T – tubules; RA – interlobar branch of the renal artery; EC – endothelial cells; L – lumen.

The immunohistochemical analysis of SOD-1 in the endothelial cells of the interlobar artery from the fructose diet group showed predominantly weak to moderate expression intensity. Stronger SOD-1 expression was also observed in the proximal and distal tubular epithelial cells (Fig. 36). Overall, the intensity of the immunohistochemical reaction was higher compared to the control group.

F+ SAM

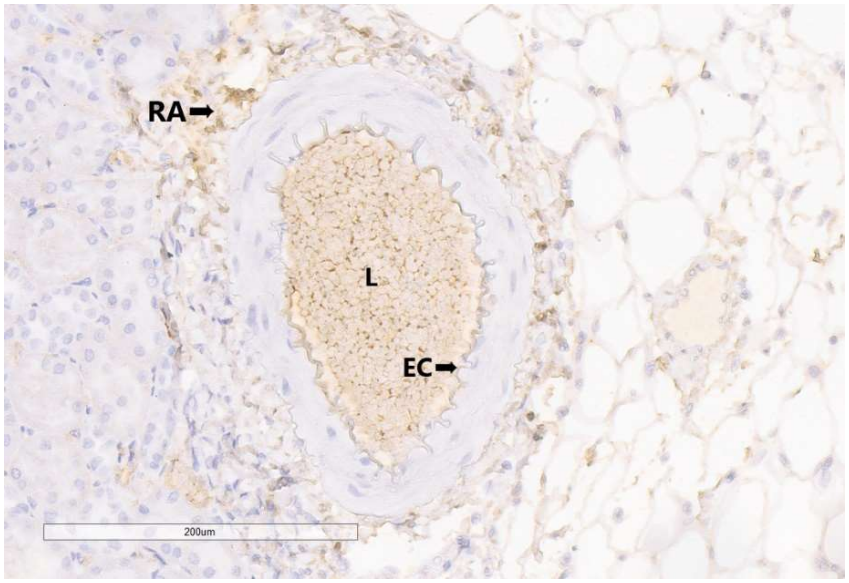

Fig. 37. Immunohistochemical analysis with anti-SOD-1 in the endothelial cells of interlobar branches of the renal artery in rats from the fructose diet group supplemented with SAM. Magnification ×4 and ×20 (Aperio Image Scope – v12.3.3.5048) Legend: F+SAM – fructose diet group with SAM supplementation; RA – interlobar branch of the renal artery; EC – endothelial cells; L – lumen

Our results show an increased expression of SOD-1 in the SAM-supplemented group. Cells with weak and moderate SOD-1 expression were observed, as well as some cells exhibiting intense expression. The intensity of the immunohistochemical reaction in the endothelial cells of this group exceeds that observed in the control group (Fig. 37).

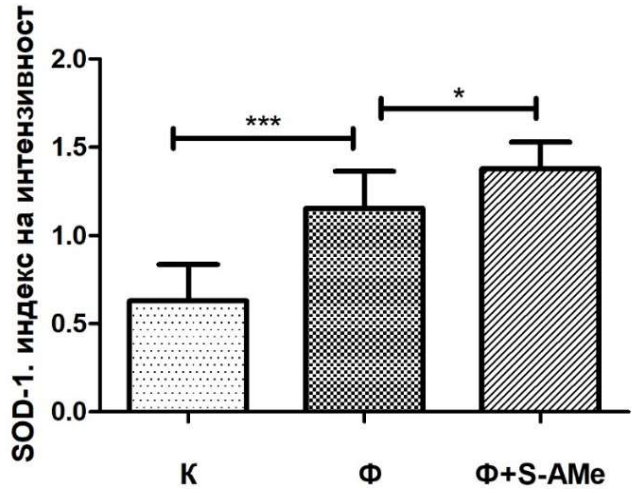

*Fig. 38. Reaction intensity index (RII) of SOD-1 in the endothelial cells of the interlobar branches of the renal artery in rats from the three experimental groups. Legend: Data are presented as mean ± standard error of the mean (SEM), (n=8); K – control group; Ф – fructose diet group; Ф+S-AMe – fructose diet group with S-AMe supplementation; * p<0.05; *** p<0.0001 – statistical significance between the control and treated groups, t-test.*

Statistically significant differences in SOD-1 expression were observed among the three groups of rats. The RII of SOD-1 expression in the fructose diet group was higher compared to the control group, with high statistical significance (***p<0.0001). Supplementation with S-AMe in rats subjected to a fructose diet resulted in a statistically significant further increase in SOD-1 expression compared to the fructose group (*p<0.05) (Fig. 38).

3.2.3 Discussion

Increasing evidence indicates that chronic fructose consumption, through excessive ROS production, contributes to the dysregulation of physiological processes and represents a leading cause of diabetes and cardiovascular diseases. Under oxidative stress, where high levels of biological oxidants disrupt the balance between oxidation and antioxidation in vivo, cellular superoxide radicals activate various apoptosis inducers either via induction of specific transcription factors or by directly causing lipid peroxidation, protein and DNA damage, and alterations in enzyme expression (Zheng M et al., 2023). Of particular importance to the pathogenic role of superoxide radicals is their ability, through activation of the NF-κB signaling pathway, to induce the expression of multiple proinflammatory mediators, such as IL-1, IL-6, TNF-α, and iNOS. Reactive oxygen species (ROS) and nitric oxide (NO), generated by iNOS, can trigger a dramatic cascade of events via the formation of peroxynitrites—highly toxic metabolites that lead to endothelial dysfunction (Dinh et al., 2014) and atherosclerosis. The interaction between ROS and proinflammatory mediators establishes a self-perpetuating cycle

linking chronic low-grade inflammation and oxidative stress.Consequently, cells rely on an innate antioxidant defense system to maintain ROS at physiologically normal levels, responsible for converting free radicals into stable forms and protecting against the harmful effects of oxidative stress.

Cu/Zn SOD (SOD1) represents a key antioxidant enzymatic system that catalyzes the dismutation of superoxide ($O_2^{\bullet -}$) into hydrogen peroxide (H_2O_2) and molecular oxygen. SOD1 is an abundant cytosolic protein, but it is also present in the mitochondrial intermembrane space (IMS). Several studies have shown that SOD1 deficiency leads to the accumulation of peroxynitrites and intracellular vascular superoxides, thereby directly contributing to enhanced myocardial oxidative stress, left ventricular hypertrophy, fibrosis, and dysfunction (Lu et al., 2008; Van et al., 2008). SOD1 accounts for 60–80% of total SOD activity in the kidneys and also plays a crucial role in the vasculature by preserving endothelial NO bioavailability (Mugge et al., 1991). SOD1 deficiency, according to Jung et al. (2003), is associated with impaired endothelial relaxation and reduced basal vascular NO levels both in vivo and in vitro (Jung et al., 2003). Furthermore, $ecSOD^{-/-}$ mice display an exaggerated hypertensive response following angiotensin II and renin induction, which can be ameliorated by in vivo treatment with an ecSOD mimetic (Jung et al., 2003). We hypothesize that fructose-induced ROS overproduction under conditions of SOD1 deficiency is the most likely mechanism leading to reduced NO bioavailability and the development of endothelial dysfunction.

The results of the immunohistochemical analysis of SOD1 expression in cardiomyocytes demonstrate a statistically significant decrease in SOD1 levels in the Fructose (Fru) group compared to the control group (Fig. 34). We hypothesize that a potential cause of this reduction in SOD1 is the overproduction of reactive oxygen species (ROS) induced by fructose overload, which excessively activates the antioxidant enzymatic system and leads to depletion of cellular antioxidants such as SOD1. In a study by Souza Cruz et al., it was shown that young adult Wistar rats (2 months old) fed a diet containing 40% sucrose for 6 months developed obesity, insulin resistance, dyslipidemia, a significant increase in hepatic MDA, and a marked decrease in SOD and glutathione levels, all of which are characteristic features of oxidative stress associated with obesity (Souza Cruz et al., 2020).

Fructose-induced hyperglycemia is of particular importance for the increased lipid peroxidation and oxidative stress observed in rats on a high-fructose diet (HFD). Prolonged exposure of rats to elevated serum glucose levels leads to a substantial accumulation of free radicals due to glucose auto-oxidation, protein glycation, and the accumulation of advanced glycation end-products (AGEs) (Nandhini et al., 2005). This, in turn, results in the depletion of antioxidant activity and a reduction in SOD1 levels. The hypothesis that antioxidant enzymes can be impaired by oxidative stress and/or glycation reactions is supported by in vitro studies, which demonstrate fructose's ability to glycate lysine residues on CnZnSOD and inactivate the enzyme (Oda et al., 1994; Yan et al., 1997; Pigeolet et al., 1990).

Unlike cardiomyocytes, the immunohistochemical analysis of SOD1 expression in the endothelial cells of the interlobar renal artery in the high-fructose diet (HFD) group was significantly higher compared to controls (Fig. 38). Notably, we observed marked expression not

only in the cytosol of the endothelial cells of the renal artery but also in the underlying smooth muscle layer and perivascular adipose tissue. We hypothesize that the elevated SOD1 levels are directly attributable to the oxidative stress and chronic low-grade inflammation induced by fructose overload, which necessitates increased SOD1 production to maintain homeostasis between excessive ROS levels and the body's antioxidant defenses.

S-Adenosyl-L-methionine (SAM), a key regulator of cellular growth, differentiation, and function, plays a critical role in protection against oxidative stress and inflammation. In our experimental model, SAM-supplemented rats exhibited a statistically significant increase in SOD1 expression both in the endothelial cells of the interlobar renal artery and in cardiomyocytes (Figs. 34, 38). Cavallaro et al. reported that SAM supplementation prevents oxidative stress by modulating GSH levels and SOD activity in TgCRND8 mice fed a vitamin B-deficient diet (Cavallaro et al., 2010). Beyond restoring mitochondrial glutathione concentrations, SAM reduces TNF-α levels and increases interleukin-10 (IL-10) expression (Purohit et al., 2007). Another study demonstrated that SAM selectively induces the apoptotic factor Bcl-xS in a time- and dose-dependent manner in HepG2 cells—but not in normal hepatocytes—via alternative splicing of Bcl-x, suggesting a mechanism by which SAM can induce apoptosis in neoplastic, but not normal, liver cells (Yang et al., 2004). Multiple studies have shown that SAM supplementation, by upregulating SOD1 expression, significantly modulates the inflammatory response and insulin resistance. This occurs through inhibition of the IKK-β/NF-κB pathway, suppression of TNF-α expression, and methylation of specific DNA sequences or proteins involved in insulin signaling (Hosea Blewett et al., 2008; Moon et al., 2010). Thus, our model demonstrates that SAM, by increasing SOD1 expression in HFD rats, protects not only against endothelial dysfunction and apoptosis but also suppresses inflammation and improves insulin signaling. These protective effects are further supported by our morphometric analysis of the left ventricle, which revealed beneficial structural effects of SAM on the left ventricular myocardium in HFD rats.

In conclusion, supplementation with SAM exerts vascular and cardioprotective effects by increasing the expression of SOD1 and NOS3 and reducing the expression of VCAM and RIP3 in HFD-fed rats.

3.3. Variations in RIP3 expression in HFD and changes following SAM supplementation

3.3.1 Results Obtained from Immunohistochemical Analysis of RIP3 Expression in Cardiomyocytes

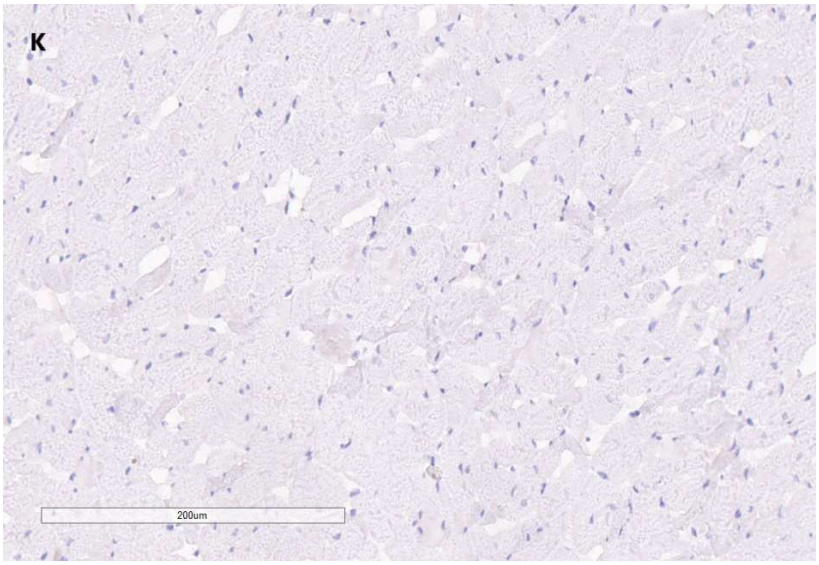

Fig. 39. Immunohistochemical staining for RIP3 in cardiomyocytes (perinuclear). Magnification ×20 (Aperio ImageScope – v12.3.3.5048) Legend: K – control group

Our results show predominantly weak to nearly absent RIP3 expression in the cardiomyocytes of the control group animals (Fig. 39).

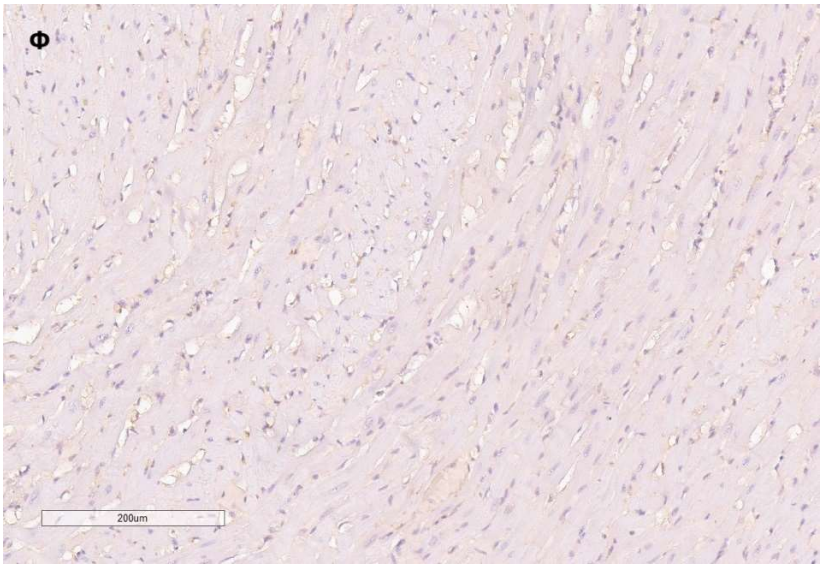

Fig. 40. Immunohistochemical analysis using anti-RIP3 in cardiomyocytes (perinuclear). Magnification ×0.20 (Aperio ImageScope – v12.3.3.5048)

Legend: Ф – fructose diet group

In contrast to the control group, the fructose diet (FD) group exhibited predominantly moderate to very intense RIP3 expression, appearing as yellow-brown cytoplasmic granules within cardiomyocytes (Fig. 40).

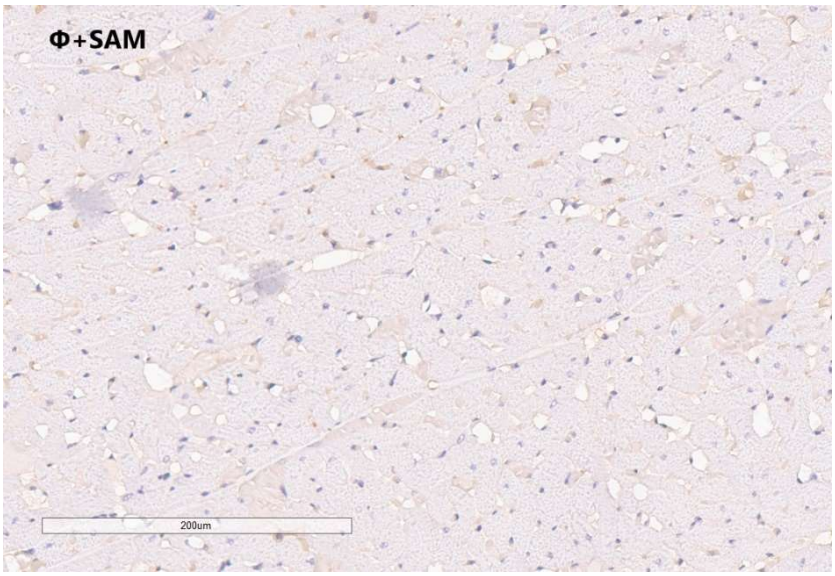

Фиг. 41. Immunohistochemical analysis using anti-RIP3 in cardiomyocytes (perinuclear). Magnification ×0.20 (Aperio ImageScope – v12.3.3.5048) Legend: Ф + SAM – fructose diet group supplemented with SAM

The immunohistochemical analysis demonstrates predominantly weak to moderate RIP3 expression in cardiomyocytes (perinuclear) of rats from the FD + SAM group, approaching the expression intensity observed in the control group. The intensity of the immunohistochemical reaction in cardiomyocytes of the supplemented group differs from that in the fructose diet group due to the observed decrease in RIP3 expression following exogenous SAM administration (Fig. 41). Figure 42 shows statistically significant differences in RIP3 expression in cardiomyocytes among the three experimental groups.

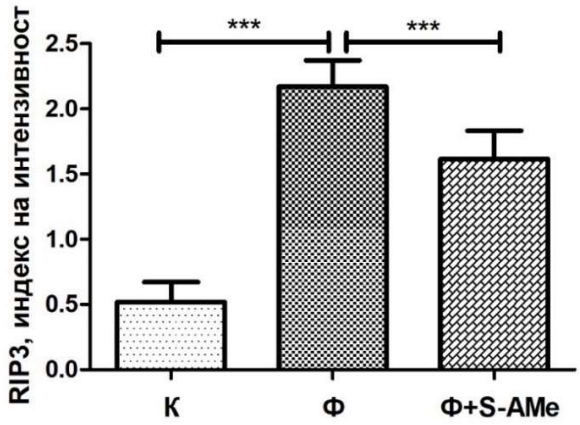

*Fig. 42. Reaction Intensity Index (RII) of RIP3 in cardiomyocytes of rats from the three experimental groups. Legend: Data are presented as mean ± standard error of the mean (SEM), (n = 8); K – control group; Ф – fructose diet group; Ф + SAMe – fructose diet and SAMe supplementation group; *** – p < 0.0001, indicating statistical significance between the control and treated groups (t-test).*

The analysis of RIP3 expression in cardiomyocytes revealed statistically significant higher levels in the fructose diet (FD) group compared to the control group (*** $p < 0.0001$). In the FD + SAMe group, RIP3 expression was significantly lower than in the FD group, also with statistical significance (*** $p < 0.0001$) (Fig. 42).

3.3.2 Results from immunohistochemical analysis of RIP3 in endothelial cells of interlobar arteries.

C

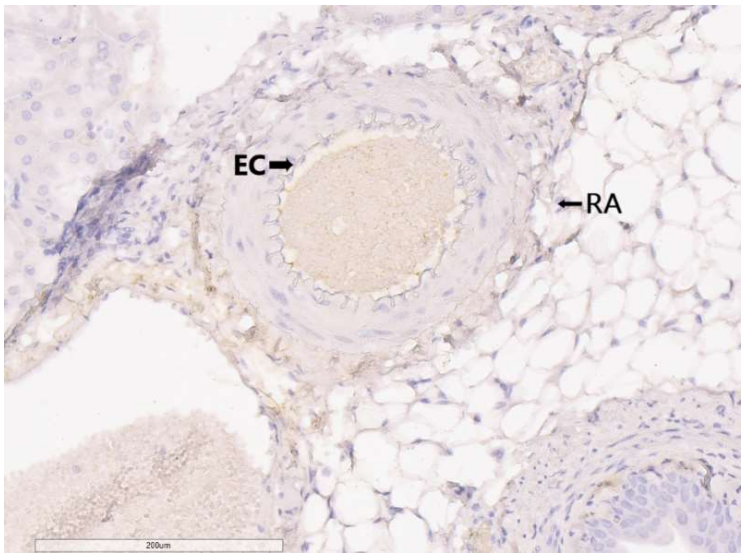

Fig. 43. Immunohistochemical staining for RIP3 in endothelial cells of the interlobar branches of the renal artery. Magnification ×0.4; ×20 (Aperio Image Scope – v12.3.3.5048)

Legend: C – control group; EC – endothelial cells; RA – interlobar branch of the renal artery

Our results demonstrate predominantly weak to nearly absent RIP3 expression in the endothelial cells of the interlobar arteries in the control group of rats (Fig. 43).

F

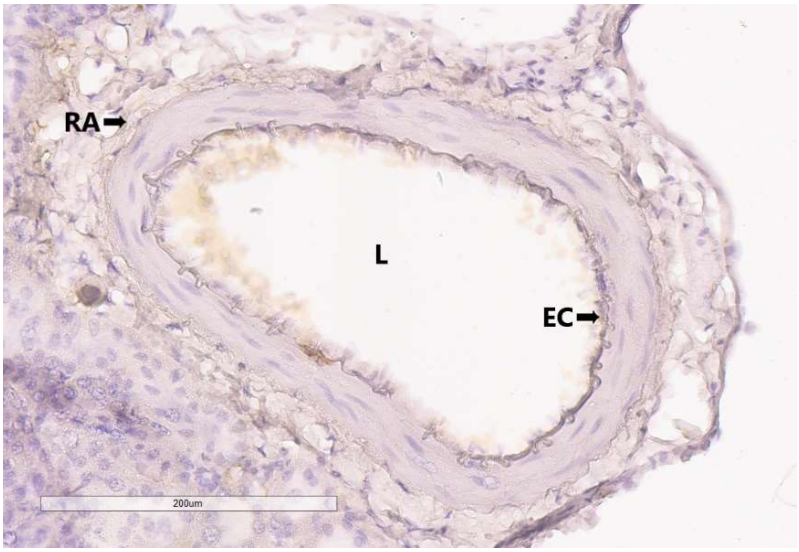

Fig. 44. Immunohistochemical analysis with anti-RIP3 in endothelial cells of the interlobar branches of the renal artery. Magnification ×0.4 and ×20 (Aperio ImageScope – v12.3.3.5048) Legend: F – fructose diet group; L – lumen; RA – interlobar branch of the renal artery; EC – endothelial cells

Our results demonstrate moderate to strong RIP3 expression, appearing as yellow-brown cytoplasmic granules in the endothelial cells of the interlobar arteries in the fructose diet group. Mild RIP3 expression is also observed in the glomeruli, particularly in proximal and distal tubular epithelial cells. The overall immunohistochemical intensity in this group is markedly higher compared to the control group, where RIP3 expression is absent (Fig. 44).

F+SAM

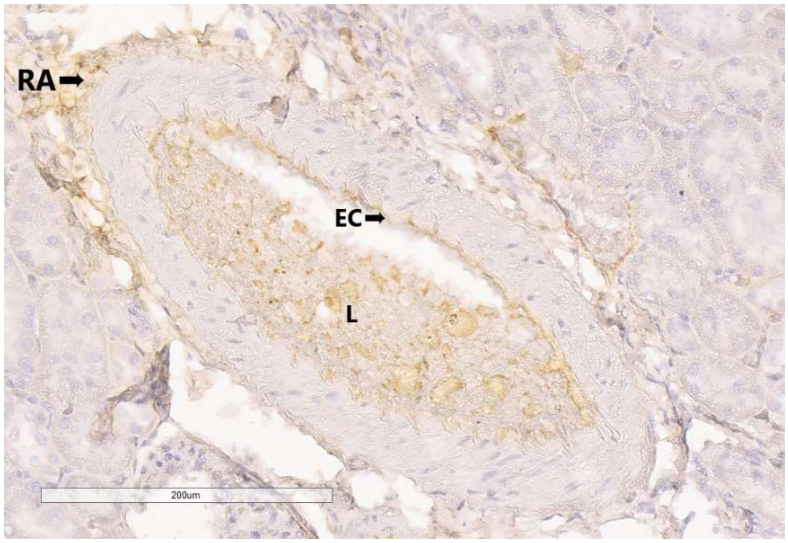

Fig. 45. Immunohistochemical staining for RIP3 in endothelial cells of the interlobar branches of the renal artery. Magnification ×0.4; ×20 (Aperio ImageScope – v12.3.3.5048) Legend: F + SAM – fructose diet rats supplemented with SAM; RA – interlobar branch of the renal artery; L – lumen; EC – endothelial cells

Our study results show a marked reduction in RIP3 expression in the FD + SAM group. Most endothelial cells exhibit weak to absent RIP3 staining. The immunohistochemical reaction intensity in the endothelial cells of the supplemented group approaches that observed in the control group (Fig. 45).

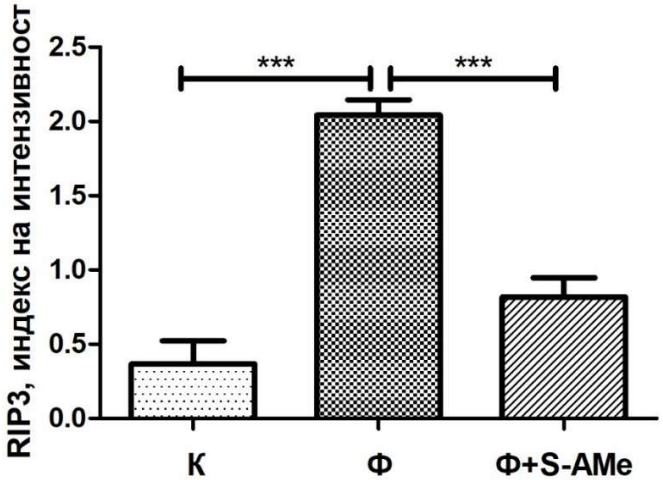

*Fig. 46. Reaction Intensity Index (RII) of RIP3 in endothelial cells of the interlobar branches of the renal artery in rats from the three experimental groups. Legend: Data are presented as mean ± standard error of the mean (SEM), (n=8); K – control group; Ф – fructose diet group; Ф+S-AMe – fructose diet group with SAM supplementation; *** $p < 0.0001$ – statistically significant difference between control and treated groups, t-test.****

Analysis of RIP3 expression in endothelial cells of the interlobar arteries revealed statistically significant higher levels in the fructose diet (FD) group compared to the control group (*** $p < 0.0001$). RIP3 expression in the FD + SAM group was significantly lower than in the FD group, also reaching statistical significance (*** $p < 0.0001$) (Fig. 46).

3.3.3 Discussion

Receptor-interacting protein kinase 3 (RIPK3 or RIP3) and mixed lineage kinase domain-like protein (MLKL) are key mediators of the programmed and regulated form of cell death known as necroptosis. RIP1-RIP3-MLKL–mediated necroptosis plays a central role in the pathogenesis of various diseases, including the progression of metabolic dysfunction–associated steatotic liver disease (MASLD) (Shojaie et al., 2020), ischemia–reperfusion injury (Jun et al., 2020), atherosclerosis, and cardiovascular diseases (Guo et al., 2022). Supporting this, studies by Wu et al. demonstrated that RIP3 kinase deficiency protects against diet-induced liver injury from high-fat and high-fructose intake (Wu et al., 2023). Other research shows that plasma RIP3 levels are significantly elevated in patients with heart failure compared to healthy individuals, and increased plasma RIP3 serves as a predictor of poor prognosis in these patients (Hu X et al., 2020).

Our results indicate that a high-fructose diet (HFD) leads to a statistically significant increase in RIP3 expression in cardiomyocytes and endothelial cells of the interlobar artery compared to controls (Figs. 42 and 46). According to multiple studies, the cardiovascular and hepatic toxicity induced by HFD is mediated through oxidative stress, which has been shown to upregulate RIP3 expression (Kanazawa et al., 2022; Jarabicová et al., 2025).

Fructose-induced obesity and the development of adipose tissue dysfunction observed in our experiment may represent a potential cause for the upregulation of RIP1-RIP3. RIP3 and pMLKL are upregulated in visceral white adipose tissue (WAT) of obese patients and show positive correlations with body mass index (BMI) and altered metabolic serum markers, such as HbA1c and insulin (Gautheron et al., 2016). Additionally, dysfunctional adipose tissue is characterized by the secretion of proinflammatory mediators, including TNFα, IFNγ, and FasL, along with their receptor molecules TNFR1, IFNR, TLR3/4, and Fas/TRAILR, which can trigger signaling cascades leading to necroptosis (Pinci et al., 2022).

It has been shown that fructose-induced oxidative stress leads to increased nuclear translocation of the transcription factor Nrf-2, reduced mitochondrial DNA, mitochondrial dysfunction, decreased activity of mitochondrial respiratory complexes, and impaired mitochondrial energy metabolism (Jaiswal et al., 2015). One of the main roles of mitochondria following pathogenic stimulation is the regulation of cell fate and the induction of necroptosis through the production of various signaling molecules.In this context, Hou et al. demonstrated that mitochondrial RIP3 interacts with the mitochondrial quality control (MQC)-related protein Drp1 to regulate mitochondrial structure and function, thereby promoting cardiomyocyte necroptosis after ischemia/reperfusion injury (Hou et al., 2018). Similarly, Luedde et al. found that RIP3 knockout suppresses cardiomyocyte necroptosis following myocardial infarction (Luedde et al., 2014).

Zhang et al. also reported that RIP3 deficiency blocks I/R (or H/R) and doxorubicin-induced myocardial necroptosis by preventing the activation of Ca^{2+}/calmodulin-dependent protein kinase (CaMKII) (Zhang et al., 2016). While the role of RIP3 in inflammation and necroptosis is well established, there is still limited evidence regarding its involvement in cardiovascular disease development. Therefore, one of the objectives of our study was to investigate whether RIP3 expression is associated with the development of myocardial hypertrophy. We observed that RIP3 expression in cardiomyocytes of rats with left ventricular hypertrophy was significantly higher compared to controls. According to Xue et al., RIP3 overexpression contributes to myocardial hypertrophy pathogenesis by promoting MLKL translocation to the plasma membrane, which further increases intracellular calcium influx (Xue et al., 2022). This calcium overload mediates many of the detrimental effects of RIP3 in cardiac remodeling through activation of the calcium-dependent phosphatase calcineurin. To confirm this mechanism, Xue et al. treated RIP3-overexpressing mice (oe-RIP3 rats) with calcium channel blockers ($LaCl_3$ and 2-APB) and demonstrated that inhibiting calcium influx reversibly attenuated RIP3-mediated cardiac remodeling (Xue et al., 2022).

The RIP3–MLKL necroptotic pathway is also implicated in the development of endothelial dysfunction and atherosclerosis. Compared to normal arteries, RIP3 and MLKL mRNA expression is significantly elevated in advanced atherosclerotic plaques, and $RIP3^{-/-}$ mice are protected from atherosclerosis development (Karunakaran et al., 2016). Fructose-induced dyslipidemia, particularly elevated oxLDL levels, upregulates the expression of necroptotic genes RIP3 and MLKL and promotes RIP3 phosphorylation, a critical step for initiating the necroptotic cell death process (Cho Y et al., 2009). Karunakaran et al. also demonstrated that oxLDL-induced necroptosis is independent of inflammasome activation, as caspase-1–deficient cells or cells treated with caspase-1 inhibitors undergo necroptotic cell death in response to oxLDL to the same extent as untreated cells (Karunakaran et al., 2016). In a separate study, Xu et al. showed that high glucose concentrations promote necroptosis and apoptosis in podocytes and increase the expression of RIPK1 and MLKL, which is observed in the kidneys of diabetic patients compared to controls (Xu et al., 2019).

Chronic fructose consumption is characterized by its ability, through multiple mechanisms such as AGE and ROS formation, upregulation of VCAM-1, and reduction of NO levels, to induce hypoxia and ultimately damage endothelial cells. Several studies indicate that endothelial RIP3 expression is naturally high in mid-stage mouse embryos, a developmental period when they are most hypoxic, before the establishment of fetal–placental circulation (Linask et al., 2014; Newton et al., 2014). Hypoxia has also been shown to increase RIPK3 expression in cultured human hepatocytes and mouse neuronal cell lines (Zhang H et al., 2021; Yang XS et al., 2017). Furthermore, several mouse models of ischemic disease show improvement on a $Ripk3^{-/-}$ background, suggesting that hypoxia-induced RIPK3 expression contributes to vascular pathology (Zhang et al., 2016; Luedde et al., 2014). Therefore, we propose that fructose consumption, via its multiple induced metabolic disturbances, directly and indirectly elevates RIP3 expression.

It is well established that increased consumption of fructose-rich foods and beverages is directly

associated with oxidative stress, insulin resistance, dyslipidemia, and cytotoxicity due to excessive production of reactive oxygen species (ROS). Mitochondrial ROS synthesis has been reported to initiate necroptosis, while activated RIP3 further promotes MLKL phosphorylation and ROS generation, forming a vicious cycle in the pathogenesis of necroptosis (Zhang Y et al., 2017). Our results demonstrate a statistically significant reduction in RIP3 expression in the SAM-supplemented group compared to the fructose diet group (Figs. 42 and 46). The administration of exogenous antioxidant SAM in our study reinforces the role of oxidative stress in necroptosis pathogenesis.

3.4. Variations in VCAM expression under a HFD and Changes Following SAM intake

3.4.1 Results from the immunohistochemical analysis of VCAM expression in the endothelial cells of the coronary arteries

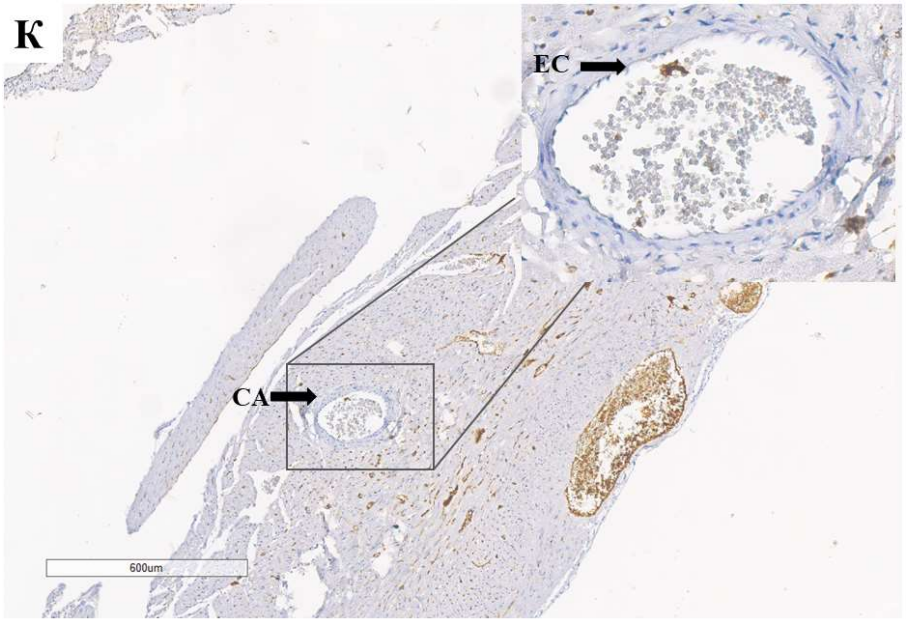

Fig. 47. Immunohistochemical analysis using anti-VCAM in the endothelial cells of coronary vessels in control group rats. Magnification ×4 and ×20 (Aperio ImageScope – v12.3.3.5048) Legend: K – control group; CA – coronary artery; EC – endothelial cells

Our results demonstrate predominantly weak to absent VCAM expression in the endothelial cells of coronary vessels in control group rats (Fig. 47).

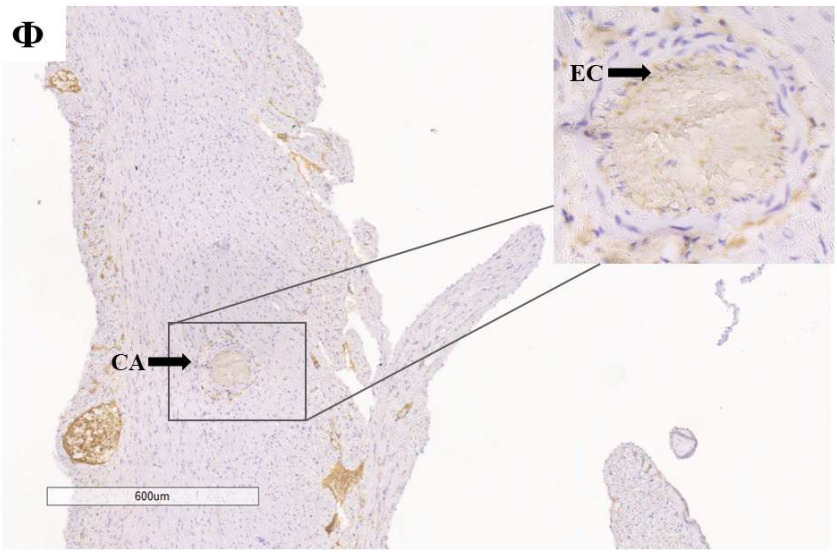

Fig. 48. Immunohistochemical analysis with anti-VCAM in the endothelial cells of coronary vessels in rats from the fructose diet (FD) group. Magnification ×4 and ×20 (Aperio Image Scope – v12.3.3.5048) Legend: Ф – fructose diet group; CA – coronary artery; EC – endothelial cells

The immunohistochemical analysis of VCAM shows predominantly moderate to strong expression in the endothelial cells of coronary vessels in the fructose diet (FD) group compared to controls (Fig. 48).

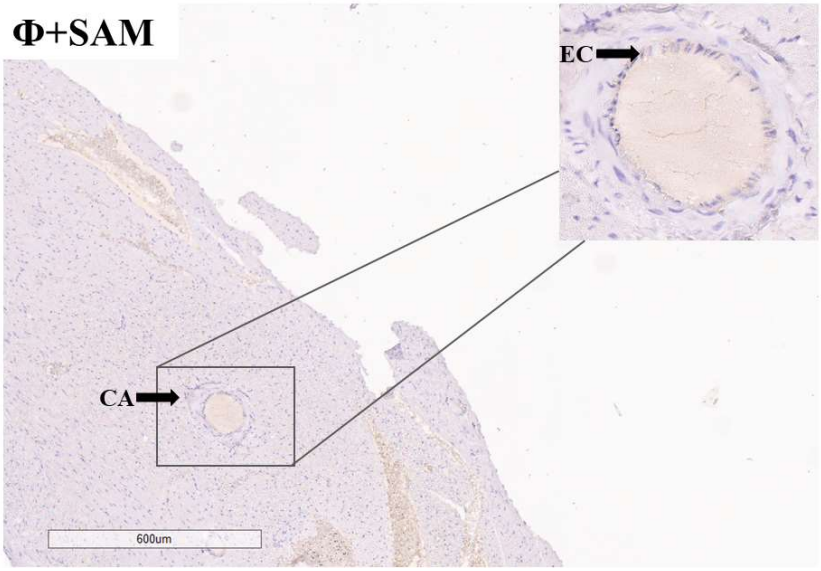

Figure 49. Immunohistochemical analysis using anti-VCAM in the endothelial cells of coronary vessels in rats from the FD + SAM group. Magnification ×8 (Aperio Image Scope – v12.3.3.5048). Legend: Ф + SAM – fructose diet with SAM supplementation; CA – coronary artery; EC – endothelial cells.

Our results show a reduction in VCAM expression in the FD + SAM group. Unlike the fructose-only group, the SAM-supplemented group predominantly exhibits cells with low VCAM expression and fewer cells with moderate expression. VCAM levels in this group approach those observed in the control group (Fig. 49). Statistical analysis revealed significant differences between the experimental groups (Fig. 50).

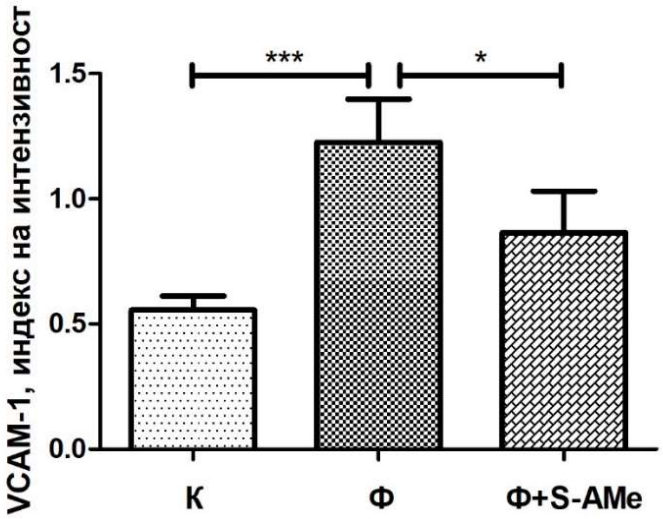

*Fig. 50. Reaction Intensity Index (RII) of VCAM in endothelial cells of coronary vessels in rats from the three experimental groups. Legend: Data are presented as mean ± standard error of the mean (SEM), (n = 8); К – control group; Ф – fructose diet group; Ф+S-AMe – fructose diet group with S-AMe supplementation; *p < 0.05; ***p < 0.0001 – statistical significance between control and treated groups, t-test.*

Endothelial VCAM expression was significantly increased in the fructose diet (FD) group compared to the control group (***$p < 0.0001$). In contrast, FD rats supplemented with S-AMe showed a statistically significant reduction in VCAM expression compared to the FD group (*$p < 0.05$) (Fig. 50).

3.4.2 Results from the immunohistochemical analysis of VCAM expression in the endothelial cells of the interlobar arteries

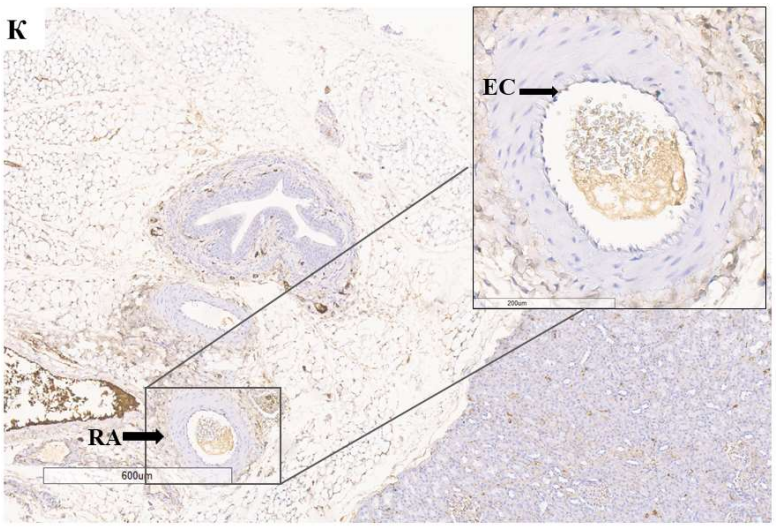

Fig. 51. Immunohistochemical analysis using anti-VCAM-1 in the endothelial cells of an interlobar branch of the renal artery. Magnification ×4 and ×20 (Aperio Image Scope – v12.3.3.5048). Legend: K – control group; RA – interlobar branch of renal artery; EC – endothelial cells.

Our results show predominantly weak VCAM expression in the endothelial cells of the renal artery in rats from the control group. A smaller number of cells exhibited absent or moderate expression compared to those with weak expression (Fig. 51).

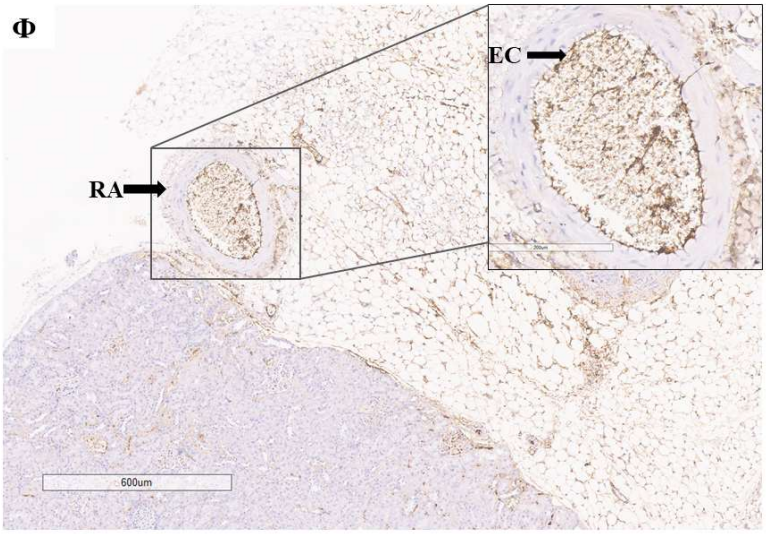

Fig. 52. Immunohistochemical analysis with anti-VCAM-1 in endothelial cells of the interlobar branch of

the renal artery. Magnification ×4 and ×20 (Aperio Image Scope – v12.3.3.5048) Legend: Ф – fructose diet rats; RA – interlobar branch of the renal artery; EC – endothelial cells

Immunohistochemical analysis of VCAM shows predominantly moderate to strong expression in the endothelial cells of the interlobar artery in the fructose diet group compared to controls (Fig. 52).

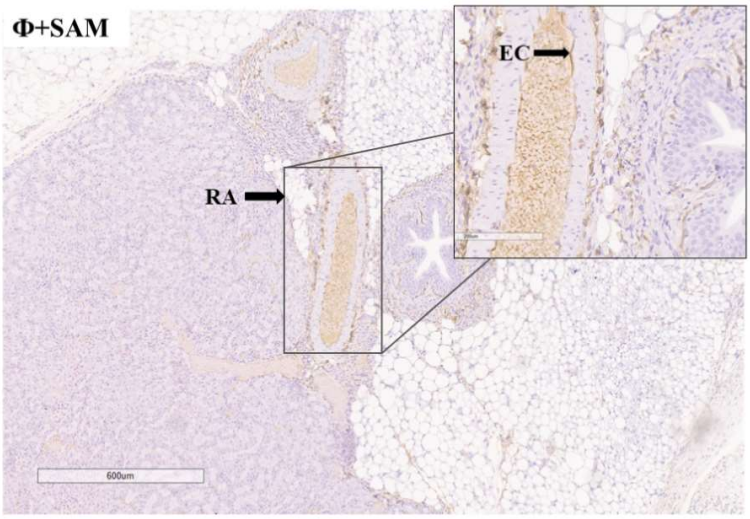

Fig. 53. Immunohistochemical analysis with anti-VCAM-1 in endothelial cells of the interlobar branch of the renal artery. Magnification ×20 (Aperio ImageScope – v12.3.3.5048) Legend: Ф+SAM – fructose diet rats supplemented with SAM; RA – interlobar branch of the renal artery; EC – endothelial cells

Our results show a reduction in VCAM expression in the FD+SAM group compared to the fructose diet group. Most endothelial cells exhibit low expression, with fewer showing moderate levels, and the overall intensity of VCAM expression approaches that observed in the control group (Fig. 53).

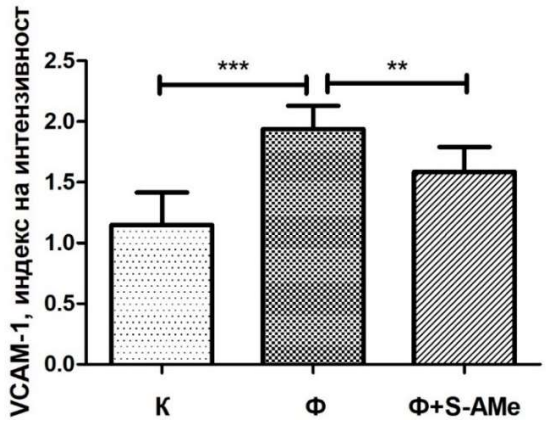

Fig. 54. Reaction Intensity Index (RII) of VCAM in endothelial cells of the interlobar branches of the renal artery in rats from the three experimental groups. Legend: Data are presented as mean ± standard error

*of the mean (SEM), (n=8); K – control group; Φ – fructose diet group; Φ+S-AMe – fructose diet group with S-AMe supplementation; **- p<0.01; ***- p<0.0001 – statistical significance between control and treated groups, t-test.*

The immunohistochemical analysis revealed a statistically significant difference in endothelial VCAM expression in the interlobar artery among the treated groups. VCAM expression was significantly higher in the fructose diet group compared to controls (*- p<0.0001). In contrast, VCAM expression was lower in rats receiving both the fructose diet and S-AMe supplementation compared to the fructose-only group, with statistical significance (- p<0.01) (Fig. 54).

3.4.3 Discussion

Inflammation plays a central role in the development of atherosclerosis and cardiovascular diseases, with studies showing that inhibiting the expression of adhesion molecules reduces plaque size in animal models, likely by decreasing monocyte recruitment from the bloodstream (Nageh et al., 1998). Vascular cell adhesion molecule-1 (VCAM-1) is a member of the immunoglobulin superfamily and was first identified as an adhesion transmembrane glycoprotein expressed on the surface of cytokine-activated endothelial cells (Osborn et al., 1989). Various pro-inflammatory cytokines (TNF-α, IL-1β, etc.), reactive oxygen species (ROS), hyperglycemia, toll-like receptor agonists, and modified LDL have been shown to induce VCAM-1 expression (Cook-Mills et al., 2011). The binding of VCAM-1 to its integrin receptor (VLA-4) mediates cellular interactions, including the recruitment of mononuclear leukocytes to vascular lesions observed in early atherosclerosis (Lavie et al., 1999), making VCAM-1 a recognized biomarker of endothelial dysfunction. During the inflammatory process, VCAM-1 activates endothelial cells, stimulates calcium influx and Rac1, which in turn further activates NADPH oxidase 2, leading to ROS generation and the development of oxidative stress (Marchese et al., 2012).

Excessive consumption of added fructose, in the form of HFCS, induces various metabolic changes that lead to low-grade chronic inflammation, oxidative stress, insulin resistance, and obesity (Basciano et al., 2005). In our study, VCAM expression was investigated to examine the relationship between adipocyte dysfunction, oxidative stress, markers of endothelial dysfunction, and low-grade chronic inflammation in an experimental obesity model.The results following high-fructose diet (HFD) administration in rats showed a statistically significant increase in VCAM expression compared to controls. In contrast, the group supplemented with SAM exhibited a statistically significant reduction in VCAM levels relative to the control group (Figs. 50, 54). These changes were observed in the endothelial cells of both coronary vessels and the interlobar artery. We hypothesize that the elevated VCAM levels are primarily driven by chronic low-grade inflammation and oxidative stress. Our findings are supported by other studies demonstrating that excessive fructose intake triggers a robust inflammatory response via the secretion of pro-inflammatory cytokines such as TNF-α, IL-1β, and others. According to Kim et al., TNF-α-activated c-Src kinase and NF-κB increase VCAM-1 expression, MCP-1, and the release of soluble ICAM-1 from osteoblast-like MC3T3-E1 cells (Kim SH et al., 2010; Tsai et al.,

2014). The elevated expression of these cytokines, in turn, promotes macrophage infiltration into adipocytes (Glushakova et al., 2008; Cook-Mills et al., 2011), further exacerbating the ongoing inflammatory process.

Vascular endothelial cells are continuously exposed to hemodynamic forces, such as shear stress imposed by blood flow (Kunsch et al., 1999). Several studies have examined the effect of fluid shear stress on endothelial function and gene expression, with some showing that shear stress alters leukocyte adhesive activity by increasing the expression of ICAM-1 and VCAM-1 (Chiu et al., 1998). Other studies demonstrate that increased blood flow and shear stress modify the redox status of endothelial cells and redox-sensitive gene expression. According to Chiu et al., shear stress–induced increases in intracellular superoxide levels, ICAM-1 mRNA, and promoter activity can be blocked by N-acetylcysteine (NAC) and superoxide dismutase (SOD) (Chiu et al., 1997), thereby reducing oxidative stress and low-grade chronic inflammation, as observed in our experimental model of fructose-induced obesity. Persistent hyperglycemia is an important risk factor that modulates vascular gene expression. Multiple authors have reported that high glucose concentrations stimulate superoxide anion generation and enhance cell-mediated LDL peroxidation in endothelial cells (Kunsch et al., 1999, et al.). Furthermore, incubation of endothelial cells with high glucose levels leads to increased activation of the NF-κB signaling pathway (Pieper et al., 1997), which upregulates the expression of adhesion molecules such as ICAM-1 and VCAM-1. NF-κB is a redox-sensitive transcription factor with a central role in vascular inflammation, activated by various inflammatory mediators, atherogenic lipoproteins, hyperglycemia, and reactive oxygen species (Zhang WJ et al., 2001). This signaling pathway is critical for vascular inflammation, as its activation under high-fructose conditions increases VCAM-1 gene expression and promotes the development of atherosclerotic plaque.

On the other hand, inflammatory mediators such as TNF-α, IL–1β, angiotensin II (Ang II), and interferon-γ activate membrane-bound NADPH oxidase and increase reactive oxygen species (ROS) production in endothelial cells (Matsubara et al., 1986). This is further supported by the study of Tummala et al., which demonstrated that treatment with diphenyleneiodonium, an NADPH oxidase inhibitor, suppresses TNF-induced superoxide production in endothelial cells (Tummala et al., 1996). The notion that ROS can function as signaling molecules to modulate vascular gene expression is also supported by observations that NADPH oxidase inhibitors block cytokine-induced VCAM-1 and ICAM-1 expression in human aortic endothelial cells and attenuate Ang II–mediated activation of VCAM-1 and MCP-1 in vascular smooth muscle cells (Chen XL et al., 1997; Tummala et al., 1996). The role of oxidative stress in regulating VCAM expression is further confirmed in our experimental model. Administration of the antioxidant SAM significantly reduced VCAM expression, highlighting the pathogenic link between oxidative stress and low-grade inflammation (figs. 50 and 54). SAM likely exerts its effects by suppressing the activity of the redox-sensitive transcription factor NF-κB, thereby reducing levels of proinflammatory mediators such as TNF-α, CRP, and VCAM in our study, which contributes to the improvement of endothelial function under fructose overload.

3.5. Changes in NOS3 expression in endothelial cells of the interlobar artery under a fructose-rich diet and following supplementation with SAM

3.5.1 Results from the immunohistochemical analysis of NOS3 expression in the endothelial cells of the interlobar arteries

C

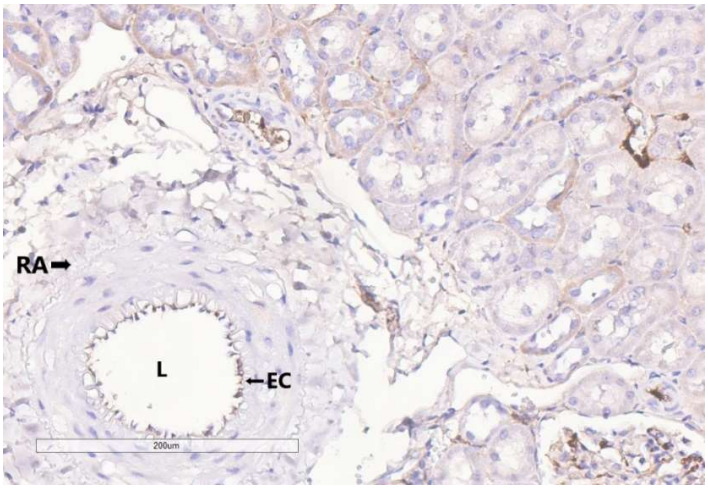

Fig. 55. Immunohistochemical analysis using anti-NOS3 in the endothelial cells of the interlobar branches of the renal artery in control group rats. Magnification ×4 and ×20 (Aperio ImageScope – v12.3.3.5048) Legend: C – control group; RA – interlobar branch of the renal artery; EC – endothelial cells; L – lumen

The immunohistochemical analysis of NOS3 in the control group demonstrates predominantly moderate to very strong expression intensity in the endothelial cells of the interlobar artery. Pronounced diffuse NOS3 expression is also observed in the tubular epithelial cells (Fig. 55).

F

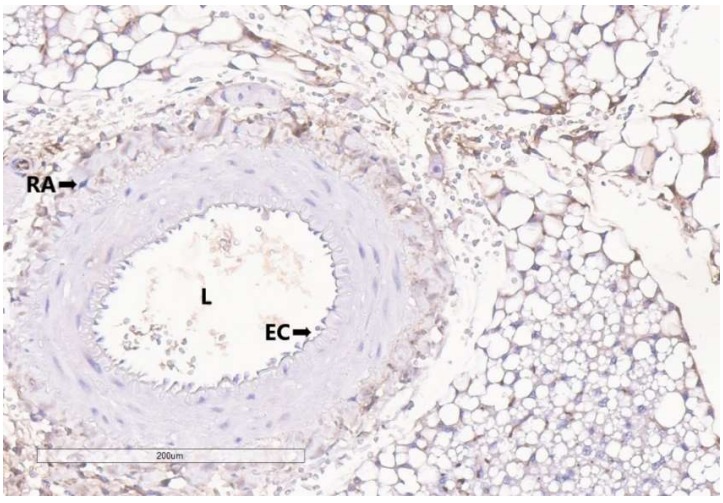

Figure 56. Immunohistochemical analysis with anti-NOS3 in the endothelial cells of the interlobar branches of the renal artery in rats from the fructose diet (FD) group. Magnification ×4 and ×20 (Aperio

Image Scope – v12.3.3.5048) Legend: F – fructose diet group; EC – endothelial cells; L – lumen; RA – interlobar branch of the renal artery

Our results show changes in NOS3 expression intensity compared to the control group. In the FD group, endothelial cells predominantly exhibit weak to absent NOS3 expression. Additionally, weak NOS3 expression is observed in the tubular epithelial cells and the surrounding adipose tissue (Fig. 56).

F+SAM

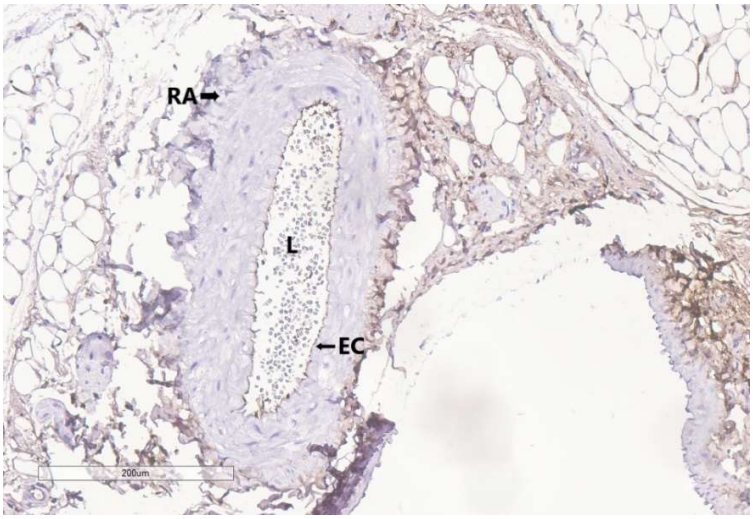

Fig. 57. Immunohistochemical analysis with anti-NOS3 in the endothelial cells of the interlobar branch of the renal artery in rats from the FD group supplemented with SAM. Magnification ×4 and ×20 (Aperio ImageScope – v12.3.3.5048)Legend: F+SAM – fructose diet group with SAM supplementation; EC – endothelial cells; RA – interlobar branch of the renal artery; L – lumen

Compared to the fructose diet (FD) group, NOS3 expression in the endothelial cells of the interlobar artery in the FD+SAM group shows a moderate to strong intensity. Moderate to low NOS3 expression is also observed in the perivascular adipose tissue (Fig. 57). The intensity of the immunohistochemical reaction in the supplemented group approaches that of the control group. Figure 58 shows statistically significant differences in NOS3 expression levels among the experimental groups.

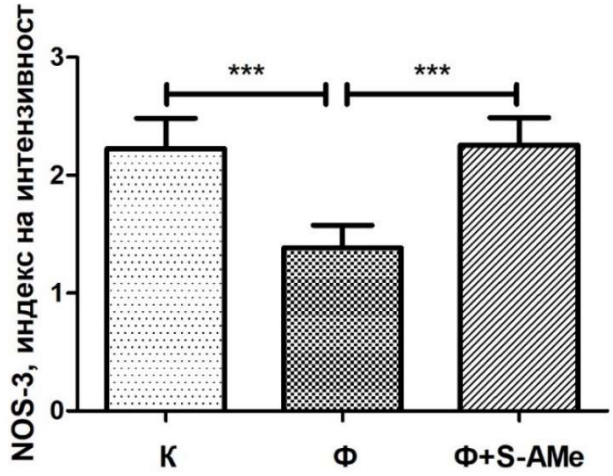

*Fig. 58. Reaction Intensity Index (RII) of NOS3 in the endothelial cells of the interlobar branch of the renal artery in rats from the three experimental groups. Legend: Data are presented as mean ± standard error of the mean (SEM), (n=8); К – control group; Ф – fructose diet group; Ф+S-AMe – fructose diet group with SAM supplementation; ***- p<0.0001 – statistical significance between the control and treated groups, t-test.*

The results of the RII analysis of NOS3 expression showed significantly lower NOS3 expression levels in the fructose diet group compared to the control group (- p<0.0001). Rats supplemented with S-AMe demonstrated significantly higher NOS3 expression levels compared to the fructose diet group (- p<0.0001) (Fig. 58).

3.5.2 Discussion

A distinctive feature of endothelial cells is their production and secretion of numerous signaling molecules that orchestrate vascular physiology, permeability, inflammation, and angiogenesis. Among these molecules, endothelial nitric oxide synthase (eNOS, NOS3) and nitric oxide (NO) stand out as key regulators, as they help maintain vascular homeostasis through local control of vascular tone and by providing antithrombotic and antioxidant effects.

Endothelial dysfunction (ED), characterized by reduced NO synthesis and decreased NO responsiveness, plays a central role in vascular imbalance, leading to a proinflammatory, prothrombotic, and oxidative state—an important component in the pathogenesis of atherosclerosis, hypertension, and cardiovascular diseases (CVD). Under physiological conditions, NOS3 is responsible for producing most of the NO, making this enzyme a critical modulator of proper cardiovascular function. This is supported by studies showing that mice with a knockout of the NOS3 gene develop arterial hypertension and have an increased risk of stroke and other cardiovascular alterations (Li H. et al., 2002).

Although NOS3 is constitutively expressed, its activity is regulated at the transcriptional, post-transcriptional, and post-translational levels by multiple stimuli (Rafikov et al., 2011). In our

experiment, we found that NOS3 expression in the endothelial cells of the renal artery in the fructose (Fru) group was significantly lower compared to the control group. On the other hand, supplementation with SAM markedly increased NOS3 expression, which was also statistically significant (Fig.64). We hypothesize that the reduction in NOS3 expression is due to the strong inflammatory response, hyperglycemia, and the development of oxidative stress associated with fructose-induced obesity.

Various mechanisms may explain the reduced expression of eNOS. It has been established that dysfunction of the eNOS–NO system is associated with oxidative changes and ROS production during fructose loading (Shinozaki et al., 1999; Glushakova et al., 2008). It is well known that NOS requires dimerization in the presence of heme and tetrahydrobiopterin (BH4) for efficient electron transfer to L-arginine. When this step is disrupted, eNOS becomes "uncoupled," functioning as a weak NADPH oxidase that produces $O_2^{\bullet -}$ instead of NO (Cyr et al., 2020), which, through its strong oxidative activity, impairs endothelial relaxation. In addition to eNOS uncoupling, reduced eNOS expression also plays a key role in decreasing NO bioavailability and in the development of endothelial dysfunction (ED), atherosclerosis, and other cardiovascular diseases. Hu et al. demonstrated a correlation between inflammatory status, endothelial dysfunction, and reduced eNOS bioavailability (Hu G et al., 2023). CRP, IL-1β, LPS, and TNF-α, key inflammatory markers, are known to reduce eNOS expression (via destabilization of eNOS mRNA) along with its bioactive functions in human aortic endothelial cells (Venugopal et al., 2002), further supporting their role in atherogenesis and vascular remodeling.

Srinivasan et al. reported that hyperglycemia also contributes significantly by reducing eNOS expression through increased mitochondrial ROS synthesis, which activates various signaling pathways, including the pro-inflammatory NF-κB and transcription factor AP-1 (Srinivasan et al., 2004). Recent studies have shown that AGEs induce oxidative stress and ED in human coronary and renal endothelial cells through activation of p38 and ERK1/2 pathways and reduced eNOS expression (Ren et al., 2017; Hu G et al., 2023). This suggests that hyperglycemia observed during fructose loading affects eNOS expression both indirectly via ROS activation and directly through endothelial damage. Conversely, Cosentino et al. reported increased eNOS expression after exposing human endothelial cells to 22 mmol/l glucose for five days (Cosentino et al., 1997). To confirm that AGE-induced oxidative stress contributes to the reduction of eNOS mRNA, we used the antioxidant SAM in our study, which led to a statistically significant increase in eNOS expression compared to the Fru group. These results demonstrate that antioxidant therapy is an effective strategy for mitigating fructose-induced vascular dysfunction.

V. CONCLUSION

In relation to the objectives and tasks set, the present study investigated the main pathophysiological mechanisms of vascular and cardiomyocyte damage under chronic fructose overload.

Within this context, an experimental model of fructose-induced obesity was established, which demonstrated that high fructose intake significantly increases the risk of developing various metabolic alterations, including hyperglycemia, dyslipidemia, chronic low-grade inflammation, oxidative stress, and insulin resistance. Our results provide compelling evidence that these changes contribute to the development of early morphological alterations in endothelial cells and cardiomyocytes, leading to impaired vascular and cardiac function. Furthermore, data from our experimental model suggest that, in fructose-induced metabolic syndrome, oxidative stress and low-grade systemic inflammation are likely functionally linked to activated necroptosis, emphasizing the need to develop and identify biomarkers for the non-invasive assessment and monitoring of necroptosis activity at the earliest stages of vascular and cardiomyocyte damage.

Our findings also show that S-AMe supplementation can effectively prevent the various changes associated with the development of metabolic syndrome induced by a high-fructose diet in rats. Supplementation with S-AMe not only reduces body weight but also improves insulin resistance, dyslipidemia, hyperglycemia, and lowers the levels of inflammatory mediators. Additionally, S-AMe reduces systemic oxidative stress and improves adipose tissue dysfunction, thereby decreasing the risk of endothelial dysfunction and various cardiovascular disorders. Based on these promising results, it can be speculated that S-AMe supplementation may improve and/or prevent some of the metabolic disturbances associated with metabolic syndrome. However, further clinical studies are needed in the future to validate our findings and to explore the potential benefits of S-AMe supplementation for human health.

VI. CONCLUSIONS

1. Administration of a high-fructose diet in rats induces changes in zoometric, biochemical, clinical-laboratory, and histological parameters that correspond to the main criteria used for the diagnosis of metabolic syndrome in humans:

1.1 Increased body weight, heart weight, and retroperitoneal fat tissue (RPFT) weight

1.2 Dyslipidemia;

1.3 Hyperglycemia and insulin resistance, evidenced by measuring the serum glucose levels and the TyG index;

1.4 Chronic low-grade inflammation, evidenced by elevated levels of TNF-α and CRP

2. The administration of a high-fructose diet in rats leads to decreased levels of vitamin D3.

3. Reduced serum vitamin D3 levels are functionally associated with the TyG index, reflecting insulin resistance and impaired lipogenesis in the high-fructose diet (HFD) group.

4. A high-fructose diet in rats induces morphological and morphometric changes in the endothelial cells of interlobar and coronary arteries, consistent with the main criteria for endothelial dysfunction.

5. A high-fructose diet in rats causes morphological and morphometric alterations in cardiomyocytes, with evidence of left ventricular hypertrophy.

6. A high-fructose diet in rats results in changes in inflammatory and antioxidant status in coronary artery endothelial cells and cardiomyocytes, demonstrated by increased VCAM-1 expression and decreased SOD1 expression.

7. A high-fructose diet in rats induces alterations in redox homeostasis as well as in inflammatory and antioxidant status, evidenced by increased VCAM-1 and SOD-1 expression and decreased NOS3 expression in the endothelial cells of the interlobar artery.

8. A high-fructose diet in rats leads to activation of necroptosis and increased RIP3 expression in endothelial cells of the interlobar artery and in cardiomyocytes.

9. Supplementation with exogenous S-AMe in rats on a high-fructose diet improves zoometric parameters, reduces perirenal adipose tissue weight, lowers levels of inflammatory markers, and increases vitamin D3 levels, thereby protecting against the development of metabolic disturbances associated with fructose-induced visceral obesity.

10. Supplementation with exogenous S-AMe in rats on a high-fructose diet enhances redox homeostasis and suppresses oxidative changes by increasing SOD-1 expression.

11. Supplementation with exogenous S-AMe in rats on a high-fructose diet inhibits the progression of activated necroptosis by reducing RIP3 expression, thereby preventing oxidative damage in endothelial cells and cardiomyocytes under conditions of fructose-induced vascular and tissue injury.

12. Supplementation with exogenous S-AMe in rats on a high-fructose diet prevents the development of endothelial dysfunction by increasing NOS3 expression and decreasing the expression of the pro-inflammatory molecule VCAM-1.

VII. CONTRIBUTIONS

1. Original contributions

1.1. A comprehensive study was conducted on the changes in the expression of SOD-1, VCAM-1, NOS3, and RIP3, and their relationship with pathomorphological alterations in the endothelial cells of coronary vessels, interlobar arteries, and cardiomyocytes in experimental animals subjected to a high-fructose diet (HFD).

1.2. A comprehensive study was conducted on the effects of SAM supplementation on morphometric and morphological parameters, as well as on the expression levels of SOD-1, VCAM-1, and NOS3 in coronary vessels, preglomerular arteries, and cardiomyocytes in experimental animals subjected to HFD.

1.3. Based on morphological results, morphometric analysis, and immunohistochemical findings, it was demonstrated that SAM administration reduces RIP3 expression in cardiomyocytes and endothelial cells of interlobar arteries in HFD rats, thereby protecting against the development of necroptotic cell death and endothelial dysfunction.

1.4. Based on clinical and laboratory investigations, it was demonstrated that SAM supplementation lowers the TyG index in fructose-induced obesity.

1.5. A functional relationship was established between the degree of reduction in serum vitamin D3 levels and the increase in the TyG index in the HFD group.

2. Confirmatory Contributions

2.1. The intake of a high-fructose diet (HFD) leads to changes in zoometric parameters, including increased body weight, retroperitoneal fat mass, and Lee index.

2.2. HFD consumption is associated with the development of oxidative stress, chronic low-grade inflammation, and endothelial dysfunction.

2.3. HFD leads to morphometric and pathomorphological changes in the left ventricular wall, manifested as thickening of the left ventricular wall.

2.4. HFD leads to morphometric and pathomorphological changes in the wall of the interlobar branches of the renal artery, expressed as wall thickening and remodeling.

3. Applied Contributions

3.1. HFD-associated metabolic disturbances, such as obesity, dyslipidemia, hyperglycemia, and insulin resistance, correspond to the diagnostic criteria for metabolic syndrome in humans. This makes our experimental model useful for studying the pathogenetic mechanisms of metabolic syndrome, as well as for developing effective therapeutic approaches for prevention, diagnosis, and treatment of this increasingly prevalent global health problem.

3.2. Supplementation with exogenous S-AMe in HFD rats reduces zoometric parameters, including body weight, retroperitoneal fat mass, Lee index, and TyG index, indicating its potential as a therapeutic agent for obesity and insulin resistance.

3.3 The antioxidant effects of exogenous S-AMe on fructose-induced morphological and morphometric changes in endothelial cells and cardiomyocytes, as well as its modulation of NOS3, VCAM-1, RIP3, and SOD-1 expression, demonstrate its potential as an effective intervention for endothelial dysfunction, oxidative damage, inflammatory responses, and necroptotic alterations associated with fructose-induced obesity.

VIII. PUBLICATIONS AND PRESENTATIONS RELATED TO THE DISSERTATION

1. Publications

1.1 Effects of melatonin supplementation on body mass index in diet-induced obesity rat model, Chivchibashi-Pavlova D., Kyuchukova D., Bekyarova G., Bratoeva K., Varna Medical Forum, 2022

1.2 New experimental models in research of the pathophysiology of cardiovascular system, Kalvachev N., Kyuchukova D., Leonidovna D., Bratoeva K., Varna Medical Forum, 2022

1.3 The involvement of necroptosis in the development of cardiovascular diseases K Bratoeva, D Kyuchukova - Varna Medical Forum, 2025

2. Participation in scientific forums

2.1 Participation in International Scientific Forums

2.1.1 Changes in hepatic fatty acid composition in experimental nonalcoholic fatty liver and S – adenosylmethionine intake. Panayotova V., Lyutfi E., Kyuchukova D., Merdzhanova A., Bratoeva K. 9-12 May 2019, 29th Annual Assembly of International Medical Association Bulgaria (IMAB), Golden Sands, Bulgaria
2.1.2 Aortic wall changes in fructose-induced obesity rat model. Chivchibashi-Pavlova Dariya, Kyuchukova Diyana, Bratoeva Kamelia. 1st International Conference of Nutritional Sciences and Dietetics – 27-29 May 2022, Thessaloniki, Greece
2.1.3 Vascular damage in fructose-induced obesity in rat model. Kyuchukova D Bratoeva K, Chivchibashi D. 30th European congress on Obesity. 17-20 May 2023 Dublin, Ireland
2.1.4 The preglomerular vasculature damage and renal dysfunction in conditions of cardio-metabolic disorders. Kameliya Bratoeva, Diyana Kyuchukova, Hristo Papanchev, Viktor V Velyanov, Nikola R Lazarov, Dariya Chivchibashi-Pavlova. FEPS&SECF Conference Granada 2024.

2.2. Participation in National Scientific Forums

2.2.1. Aortic wall and periaortic adipose tissue changes in obese rats supplemented with melatonin, Chivchibashi-Pavlova Dariya, Kyuchukova Diyana, Stoyanov Georgi, Bratoeva Kameliya, National Congress on Physiology with International Participation. Stara Zagora Mineral Baths, Spa Hotel Armira, Bulgaria. 30 October – 1 November 2022

IX. ACKNOWLEDGEMENTS

I would like to express my heartfelt gratitude to:

- Assoc. Prof. Dr. Kamelia Bratoeva, MD, my scientific supervisor, for her invaluable professional guidance, patience, responsiveness, and unwavering support throughout the development of this dissertation.

- My colleagues from the Department of Pathophysiology, for their continuous support and collaboration.

- Laboratory assistants Velina Kenovska (Department of Anatomy and Cell Biology), Ginka Vangelova, and Zornitsa Georgieva (Department of Physiology and Pathophysiology / Department of Pathophysiology) for their invaluable help and expert advice in the preparation of histological and immunohistochemical specimens.

- Dr. Daria Leonidovna Chivchibashi-Pavlova (Department of General and Clinical Pathology, Forensic Medicine and Deontology) for her professional guidance in performing the immunohistochemical analyses, as well as her support and valuable advice during the development of this dissertation.

- I sincerely thank my family for their unconditional support, patience, understanding, and moral encouragement throughout my studies and the preparation of this dissertation.